การศึกษาการแสดงออกของโปรตีนจำเพาะในสมอง ก้านสมอง และไขสันหลังของสุนัขที่เป็นโรคพิษสุนัขบ้า

นางสาวณัฐภาณินี ถนอมศรีเดชชัย

วิทยานิพนธ์นี้เป็นส่วนหนึ่งของการศึกษาตามหลักสูตรปริญญาวิทยาศาสตรดุษฎีบัณฑิต
สาขาวิชาชีวเวชศาสตร์ (สหสาขาวิชา)
บัณฑิตวิทยาลัย จุฬาลงกรณ์มหาวิทยาลัย
ปีการศึกษา 2553

ลิขสิทธิ์ของจุฬาลงกรณ์มหาวิทยาลัย

EXPRESSION OF SPECIFIC PROTEIN(S) IN BRAIN, BRAINSTEM AND SPINAL CORD OF RABIES INFECTED DOGS

Miss Natthapaninee Thanomsridetchai

A Dissertation Submitted in Partial Fulfillment of the Requirements
for the Degree of Doctor of Philosophy Program in Biomedical Sciences
(Interdisciplinary Program)
Graduate School
Chulalongkorn University
Academic Year 2010
Copyright of Chulalongkorn University

Thesis Title	EXPRESSION OF SPECIFIC PROTEIN(S) IN BRAIN, BRAINSTEM AND SPINAL CORD OF RABIES INFECTED DOGS
By	Miss Natthapaninee Thanomsridetchai
Field of Study	Biomedical Sciences
Thesis Advisor	Professor Thiravat Hemachudha, M.D.
Thesis Co-advisor	Sittiruk Roytrakul, Ph.D.

Accepted by the Faculty of Graduate School, Chulalongkorn University in Partial Fulfillment of the Requirements for the Doctoral Degree

..... Dean of the Graduate School

(Associate Professor Pornpote Piumsomboon, Ph.D.)

THESIS COMMITTEE

..... Chairman

(Professor Apiwat Mutirangura, M.D., Ph.D.)

..... Thesis Advisor

(Professor Thiravat Hemachudha, M.D.)

Sittiruk Roytrakul ..... Thesis Co-advisor

(Sittiruk Roytrakul, Ph.D.)

..... Examiner

(Professor Teerapong Tantawichien, M.D.)

..... Examiner

(Professor Shanop Shuangshoti, M.D.)

Pakamatz Khawplod ..... External Examiner

(Pakamatz Khawplod, Ph.D.)

ณัฐภาณินี ถนอมศรีเดชชัย: การศึกษาการแสดงออกของโปรตีนจำเพาะในสมอง ก้านสมอง และไขสันหลังของสุนัขที่เป็นโรคพิษสุนัขบ้า (EXPRESSION OF SPECIFIC PROTEIN(S) IN BRAIN, BRAINSTEM AND SPINAL CORD OF RABIES INFECTED DOGS) อ.ที่ปรึกษาวิทยานิพนธ์หลัก: ศ.นพ.ธีระวัฒน์ เหมะจุฑา, อ. ที่ปรึกษาวิทยานิพนธ์ร่วม: ดร.สิทธิรักษ์ รอยตระกูล, 81 หน้า.

โรคพิษสุนัขบ้าทั้งในคนและในสุนัขมีอาการแสดงคล้ายคลึงกัน 2 แบบ คือ แบบดุร้ายและแบบอัมพาต แม้จะมีการศึกษาจำนวนมากก่อนหน้านี้ แต่ก็ยังไม่ทราบถึงกลไกการเกิดโรคที่แน่ชัด ในการศึกษาครั้งนี้จึงใช้เทคนิคโปรตีโอมิกส์ เพื่อศึกษาการเปลี่ยนแปลงระดับการแสดงออกของโปรตีนในสมองส่วนฮิปโปแคมปัส ก้านสมอง และไขสันหลังของสุนัขที่เป็นโรคพิษสุนัขบ้าทั้งที่มีอาการแบบดุร้ายและแบบอัมพาตที่ติดเชื้อโดยธรรมชาติ โดยเปรียบเทียบกับสุนัขที่ไม่ได้เป็นโรคพิษสุนัขบ้าที่ส่งมาตรวจที่สถานเสาวภา สภากาชาดไทย ดำเนินการทดลองโดยสกัดโปรตีนจากเนื้อเยื่อ จากนั้นนำมาแยกในโพลีอคริลาไมด์เจลแบบสองมิติร่วมกับวิธีแมสสเปกโตรเมทรี ทำการยืนยันผลการแสดงออกของโปรตีนบางตัวด้วยวิธีเรียลไทม์พีซีอาร์ ผลการศึกษาพบว่ามีจุดโปรตีนที่มีการเปลี่ยนแปลงระดับการแสดงออกเพื่อตอบสนองต่อการติดเชื้อมากกว่า 1,000 จุด เมื่อนำมาวิเคราะห์ทางสถิติ พบว่ามีจำนวนจุดโปรตีนที่มีการแสดงออกเปลี่ยนแปลงแตกต่างกันอย่างมีนัยสำคัญทางสถิติจำนวน 32, 49 และ 67 จุดโปรตีนจากในสมองส่วนฮิปโปแคมปัส ก้านสมอง และไขสันหลังตามลำดับ ซึ่งเมื่อนำโปรตีนที่พบมาจัดแบ่งกลุ่มตามหน้าที่ ได้แก่ โปรตีนในกลุ่มที่เกี่ยวข้องกับการตอบสนองในสภาวะต่างๆ, โปรตีนโครงสร้างค้ำจุน, เอนไซม์, การควบคุมการเจริญเติบโต, การตาย เป็นต้น จากโปรตีนทั้งหมดที่ได้ พบว่ามีจุดโปรตีน มีการแสดงออกที่เปลี่ยนแปลงอย่างมีนัยสำคัญทางสถิติเมื่อเปรียบเทียบระหว่างกลุ่มอาการแบบดุร้ายและแบบอัมพาต ในสมองส่วนฮิปโปแคมปัส 13 จุด ก้านสมอง 17 จุด และไขสันหลัง 41 จุด การศึกษานี้เป็นการศึกษาแรกที่ศึกษาในตัวอย่างที่ติดเชื้อโรคพิษสุนัขบ้าโดยธรรมชาติ ดังนั้นการศึกษาในครั้งนี้จะช่วยให้มีการพัฒนาองค์ความรู้นำมาวิเคราะห์ต่อไปว่าโปรตีนที่ต่างกันอยู่ในกระบวนการของการตายในระดับใด หรือไม่ หรือเกี่ยวกับกลไกที่เกี่ยวข้องกับการเพิ่มจำนวนของไวรัส เป็นต้น อันจะเป็นข้อมูลสำคัญสำหรับการศึกษาต่อไปในอนาคต ซึ่งจะนำไปสู่การอธิบายกลไกการทำงาน การทำอันตราย การประยุกต์ใช้ในการรักษาต่อไป

สาขาวิชา ชีวเวชศาสตร์ ..... ลายมือชื่อนิสิต ณัฐภาณินี ถนอมศรีเดชชัย .....

ปีการศึกษา 2553 ..... ลายมือชื่อ อ.ที่ปรึกษาวิทยานิพนธ์หลัก .....

ลายมือชื่อ อ.ที่ปรึกษาวิทยานิพนธ์ร่วม สิทธิรักษ์ รอยตระกูล .....

4989664420: MAJOR BIOMEDICAL SCIENCES

KEYWORD: BRAINSTEM / FURIOUS/ HIPPOCAMPUS/ PARALYTIC/ PROTEOMICS/ RABIES/ SPINAL CORD

NATTHAPANINEE THANOMSRIDETCHAI: EXPRESSION OF SPECIFIC PROTEIN(S) IN BRAIN, BRAINSTEM AND SPINAL CORD OF RABIES INFECTED DOGS. ADVISOR: PROF. THIRAVAT HEMACHUDHA, M.D. CO-ADVISOR: SITTIRUK ROYTRAKUL, Ph.D., 81 pp.

Furious and paralytic forms of rabies are unique clinical entities. They have been recognized particularly in rabies infected humans and dogs. The underlying mechanisms remained unclear. . We investigated host responses as determined by changes in the cellular proteome of nervous tissue samples from naturally rabies infected furious and paralytic dogs during late stage as compared to non-infected controls. Proteins were extracted from these tissues and analyzed by two-dimensional gel electrophoresis (2-DE). These proteins were then identified by quadrupole time-of-flight mass spectrometry and tandem mass spectrometry (Q-TOF MS and MS/MS) and were validated by real-time PCR. From >1,000 protein spots visualized in each gel, spot matching, quantitative intensity analysis and ANOVA with Tukey's post-hoc multiple comparisons revealed 32, 49 and 67 protein spots that were differentially expressed among the three clinical groups in hippocampus, brainstem and spinal cord, respectively., including anti-oxidants, apoptosis-related proteins, cytoskeletal proteins, heat shock proteins/ chaperones, immune regulatory proteins, metabolic enzymes, neuron-specific proteins, transcription/translation regulators, ubiquitination/proteasome-related proteins, vesicular transport proteins, and hypothetical proteins. Among these, 13, 17 and 41 proteins in hippocampus, brainstem and spinal cord, respectively, significantly differed between paralytic and furious forms, and thus may potentially be biomarkers to differentiate these two distinct forms of rabies. In summary, we report herein for the first time a large dataset of changes in proteomes of hippocampus, brainstem and spinal cord in dogs naturally infected with rabies. These data will be useful for better understanding of molecular mechanisms of rabies and for differentiation of its paralytic and furious forms.

Field of Study :Biomedical Sciences Student's Signature Natthapaninee Thanomsridetchai

Academic Year : 2010 Advisor's Signature

Co-advisor's Signature Sittiruk Roytrakul

ACKNOWLEDGEMENTS

I would therefore firstly express my deepest and sincere gratitude to my advisor Professor Thiravat Hemachudha and my co-advisor Dr.Sittiruk Roytrakul from Proteomics Research Laboratory, BIOTEC, Genome Institute, NSTDA for giving me one of the most important opportunities in my life and providing constant support, including giving advises and guidances.

I am deeply grateful to my thesis examination committee Professor Dr. Apiwat Mutirangura, Professor Teerapong Tantawichien, Professor Shanop Shuangshoti and Dr.Pakamatz Khawplod who gave me valuable comments, suggestions, and encouragement essential for the successful completion of this thesis.

The work in this thesis has been completed with the help from Dr. Visith Thongboonkerd and all members of Medical Proteomics Unit, Office for Research and Development, Faculty of Medicine, Siriraj Hospital, Mahidol University, who has given me the kindly helpfulness.

I would like to special thank for Mr.Veera Tepsumethanon, D.V.M. (Chief of Clinical Service Department Rabies Diagnosis and Post exposure Treatment, Queen Saovabha Memorial Institute, Thai Red Cross Society) and all staff for their helpful in providing samples for my thesis experiment.

I am extremely grateful to Dr. Supaporn Wacharapluesadee for her valuable technical advice and I also would like to express my deepest appreciation and thankfulness to all members of Molecular Biology Laboratory for Neurological Diseases, WHO-CC for Research and Training on Viral Zoonoses, Faculty of Medicine, Chulalongkorn University for their friendship and encouragement.

I wish to thank many other people left unnamed for their helpfulness.

Finally, I would like to give whole heart to my aunt for her understanding and supported mentally during the course of this work. Without her encouragement, this study would not have been completed.

I gratefully acknowledge the financial support from:

- Graduate thesis grant from Biomedical Sciences program
- Teaching assistance fellowship from Graduate School
- National Center for Genetic Engineering and Biotechnology (BIOTEC), the National Science and Technology Development Agency (Thailand)

CONTENTS

LIST OF TABLES

Table **Page**

LIST OF FIGURES

Figure **Page**

LIST OF ABBREVIATIONS

2-DE	two-dimensional gel electrophoresis
AIF	apoptosis-inducing factor
ANOVA	one-way analysis of variance
AT3	rat prostatic adenocarcinoma cells
Bax	Bcl-2 associated X protein
Bcl-2	B-cell lymphoma 2
CDC	Centers for Disease Control and Prevention
cNOS	constitutive nitric oxide synthase
CNS	central nervous system
CSF	cerebrospinal fluid
CVS	challenged virus standard
DNA	deoxyribo Nucleic Acid
DRG	dorsal root ganglion
EM	electron microscope
eNOS	endothelial nitric oxide synthase
ERA	Evelyn Rotnycki Abelseth
G protein	glycoprotein
ICE	caspase 1
iNOS	inducible nitric oxide synthase
kb	kilobase
kDa	kilo Daltons
L protein	RNA-dependent RNA polymerase or large protein
LM	light Microscope
M protein	matrix protein
MALDI Q-TOF	matrix-assisted laser desorption/ionization quadrupole time-of-flight mass spectrometry
MRI	magnetic resonance imaging
mRNA	massenger Ribonucleic Acid
N protein	nucleocapsid

nNOS	neuronal nitric oxide synthase
NO	nitric oxide
NOS	nitric oxide synthase
P protein	phosphoprotein
PARP	poly ADP-ribose polymerase
PCR	Polymerase Chain Reaction
RNP	ribonucleoprotein complex
RV	Rabies virus
SHBRV	silver-haired bat rabies virus
TUNEL	terminal deoxynucleotidyl transferase (TdT)-mediated dUTP nick-end-labeling

CHAPTER I
INTRODUCTION

1. Background and Rationale

Rabies remains an enigma. Almost a universally fatal outcome is expected once symptoms and signs develop. Three survivors with non-significant sequelae or none at all have been reported and associated with bat variants (Hattwick et al., 1972; Willoughby et al., 2005; Centers for Disease Control and Prevention (CDC)., 2010). Human patients associated with dog variants exhibited more unique clinical manifestations than those with bats in the form of furious and paralytic rabies. A more pronounced suppression of immune response to rabies virus has been shown in dog- than bat-related cases (Hemachudha et al., 2002). None of the cases associated with dog viruses in Thailand, Cambodia and Africa were cerebrospinal fluid (CSF) positive for rabies antibody (Hemachudha et al., 2000; Dacheux et al., 2008). The development of serum rabies antibody is also unpredictable as compared to the bat related cases. Serum and CSF rabies antibody appeared with time of survival in the latter (Hemachudha, 1994).

Rabies in humans can be categorized in two forms: classic (furious and paralytic rabies) and non-classic or atypical rabies. All forms are progressive to coma and death usually within 14 days without intensive care support (Hemachudha et al., 2002). The majority of the cases present as furious rabies, with hydrophobia and hyper-excitability. Paralytic rabies present with flaccid muscle weakness. The pathogenesis underlying these two clinical forms remains to be elucidated. The non-classic or atypical rabies usually occurs following exposure to the bite of a bat, but has also been described in association with dog variants whereas the classic form is associated with dog variants (Hemachudha et al., 2006). The two classical forms of rabies share a similar pattern of regional viral antigen distribution in the central nervous

system (CNS) with a predilection of brainstem and spinal cord during the early clinical phase. Analysis of the nucleocapsid (N) and glycoprotein (G) and phosphoprotein (P) genes of rabies viruses from 2 furious and 2 paralytic rabies patients demonstrated no specific genetic or amino-acid pattern (Hemachudha et al., 2003). Both furious and paralytic rabies patients remain alert until the pre-terminal stage; functions of brainstem remain intact almost throughout the whole course or until the pre-terminal phase. Analysis of regional distribution of rabies viral antigen in the CNS of human rabies patients of both forms revealed similar pattern. The site of the infecting bites in these patients did not have any influence on the distribution of antigen. Rabies viral antigen preferentially localized in the spinal cord and brainstem and basal ganglia and thalamus if the survival period was less than 7 days.

Similar findings were found in magnetic resonance imaging (MRI) study; spinal cord, brainstem and midline structures were involved predominantly in both forms. It has been shown that limb weakness in paralytic rabies patient was explained by peripheral nerve dysfunction based on serial electrophysiologic examination prior to coma stage (Laothamatas et al., 2003). In case of non comatose furious rabies patients, anterior horn cell dysfunction in the spinal cord can be observed. These patients do not exhibit any demonstrable weakness of the arms and legs. Innate immune responses in the brains of paralytic dogs have been greater than furious dogs which inversely correlated with the viral amount in the brains. Disturbances of MRI signals in the brains are greater in the case of paralytic than furious rabies infected patients and dogs (Laothamatas et al., 2003, 2008). The faster time to death is also another characteristic of furious rabies. Despite dissimilarity among clinical manifestations, imaging features, clinical courses and amount of viral load in the brain, they share similar pathologies of the CNS, including scant inflammation (Hemachudha et al., 2002; Laothamatas et al., 2003; Mitrabhakdi et al., 2005). Inflammation may be truly lacking or invading cells became

apoptotic, thus, unable to be demonstrated (Laothamatas et al., 2003; Mitrabhakdi et al., 2005).

Preservation of the integrity of infected neurons is essential for the virus to propagate from periphery to the CNS, particularly spinal cord and brainstem pathways. The pathogenicity of a particular strain correlates inversely with its ability to induce apoptosis. Apoptosis may be a protective rather than a pathogenetic mechanism, less pathogenic viruses induced more apoptosis than more pathogenic viruses. Lack of apoptosis in the CNS has been shown to be a marker for virulence of wild-type or street rabies virus in order to escape immune recognition and to facilitate spreading (Yan et al., 2001; Sarmento et al., 2005 ; Jackson et al., 2008 ; Suja et al., 2009 ; Préhaud et al., 2010).

In contrast, fixed virus, such as the challenged virus standard (CVS) strain, induces marked degree of apoptosis in the infected neurons (Jackson et al., 1997, 1998; Morimoto et al., 1999; Weli et al., 2006). Intriguingly, neurons of different regions display diverse degrees of resistance to cell death. It has been demonstrated that motor neurons of spinal cord resist to apoptosis and cytolysis, and remain functioning several days after CVS infection. However, hippocampal neurons become apoptotic shortly after the infection (Guigoni and Coulon, 2002). Midline CNS structures, i.e. thalamus, brainstem, basal ganglia and spinal cord, have been shown to be preferentially infected with rabies in both humans and dogs (Tirawatnpong et al., 1989; Laothamatas et al., 2003, 2008). Therefore, the survival of neurons may depend not only on the viral strain but also on differential site-specific responses.

In this study, naturally rabies infected dogs, both furious and paralytic forms, were used for proteomics analysis. Three regions of CNS; hippocampus, brainstem and spinal cord, were compared by Two-dimensional gel electrophoresis (2-DE) combined with MALDI quadrupole time-of-flight (MALDI Q-TOF) mass spectrometry. Site-specific responses were analyzed.

Hopefully, a greater understanding of the host responses and effect of viral infection upon neurophysiology and homeostasis will be achieved. The study will be performed in suitable experimented model. Result of the study may provide insights into the pathogenesis mechanisms, by which viral infection leads to disease development and may explain different clinical characteristics between furious and paralytic rabies.

2. Research Question

Are there any differences in the expression of protein(s) in brain, brainstem and spinal cord of rabies infected dogs based on proteomic study?

3. Objective of the Study

To display and analyze in the expression of protein(s) in brain, brainstem and spinal cord of rabies infected and non-rabies infected dogs.

4. Hypothesis

There are differences in the expression of protein(s) in brain, brainstem and spinal cord of furious and paralytic dogs.

5. Key Words

Brainstem; Furious; Hippocampus; Paralytic; Proteomics; Rabies; Spinal cord

6. Expected Benefits and Applications

This is proof that there are alterations or differences in the expression of protein(s) that is (are) specific in brain, brainstem and spinal cord of furious

and paralytic rabies infected dogs, compared to non-rabies infected group. The result of this study should also demonstrate how host responds to viral infection which may lead to pathogenetic mechanisms.

CHAPTER II
LITERATURE REVIEW

Genomic organization of rabies virus

Rabies virus (RV) is a highly neurotropic virus that is classified in the Rhabdoviridae family of the Mononegavirale order of viruses. It is further divided into the Lyssavirus genus (Murphy et al., 1995). The negative, single-stranded genome is nonsegmented RNA that is approximately 12 kb (Mayo and Pringle, 1997). The rabies genome encodes 5 structural proteins of the virus particle (virion) include: nucleoprotein (N), phosphoprotein (P), matrix protein (M), glycoprotein (G) and RNA-dependent RNA polymerase or large protein (L). The ribonucleoprotein complex (RNP) is composed of the genomic RNA intimately associated with N, L and P proteins. This complex ensures a functional template for transcription and replication. A layer of M protein covers this complex structure. The glycoprotein forms are tightly arranged above the virion surface (CDC).

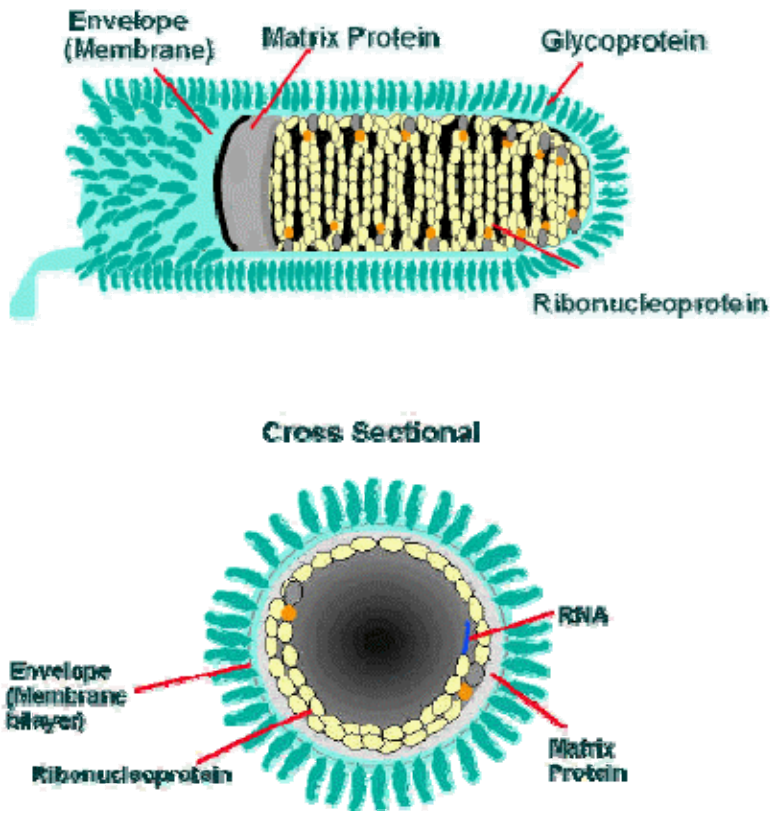

Figure 1. Structure of rabies virus (CDC)

Pathogenesis of rabies virus

Rabies virus is transmitted via the bite of a rabid animal which shed infectious virus with their saliva. Rabies virus enters the body through transdermal inoculation (i.e. wounds) or direct contact of infectious material (i.e. saliva, cerebrospinal liquid, nerve tissue) to mucous membranes or skin lesions. The virus remains close to the site of exposure for the majority of the long incubation period, which usually lasts from less than 7 days to more than 6 years (Smith et al., 1991) depending on the amount of virus in the saliva, the site of inoculation and the virus strain. After entry, rabies virus binds to the nicotinic acetylcholine receptor in muscle (Lentz et al., 1982), which is expressed on the postsynaptic membrane of the neuromuscular junction. After budding from the plasma membrane of muscle cell, virus is taken up into

unmyelinated nerve endings at the neuromuscular junctions or at the muscle spindles.Viruses may replicate within striated muscle cells or directly infect nerve cells (Murphy and Bauer, 1974). The virus then travels to CNS via retrograde fast axonal transport at 8 to 20 mm/day mechanisms (Wilson et al., 1975). Both motor and sensory fibres may be involved depending on the animal infected (Murphy, 1977). Once the virus has reached the CNS, rapid virus replication takes place, causing pathologic effects on nerve cell. The virus then moves from the CNS via anterograde axoplasmic flow within peripheral nerves, leading to centrifugal spread along peripheral nerves to other tissue, such as salivary glands, liver, muscle, skin, adrenal glands, and heart. Rabies virus replications in acinar cells of salivary glands result in viral excretion in the saliva of rabid animals.

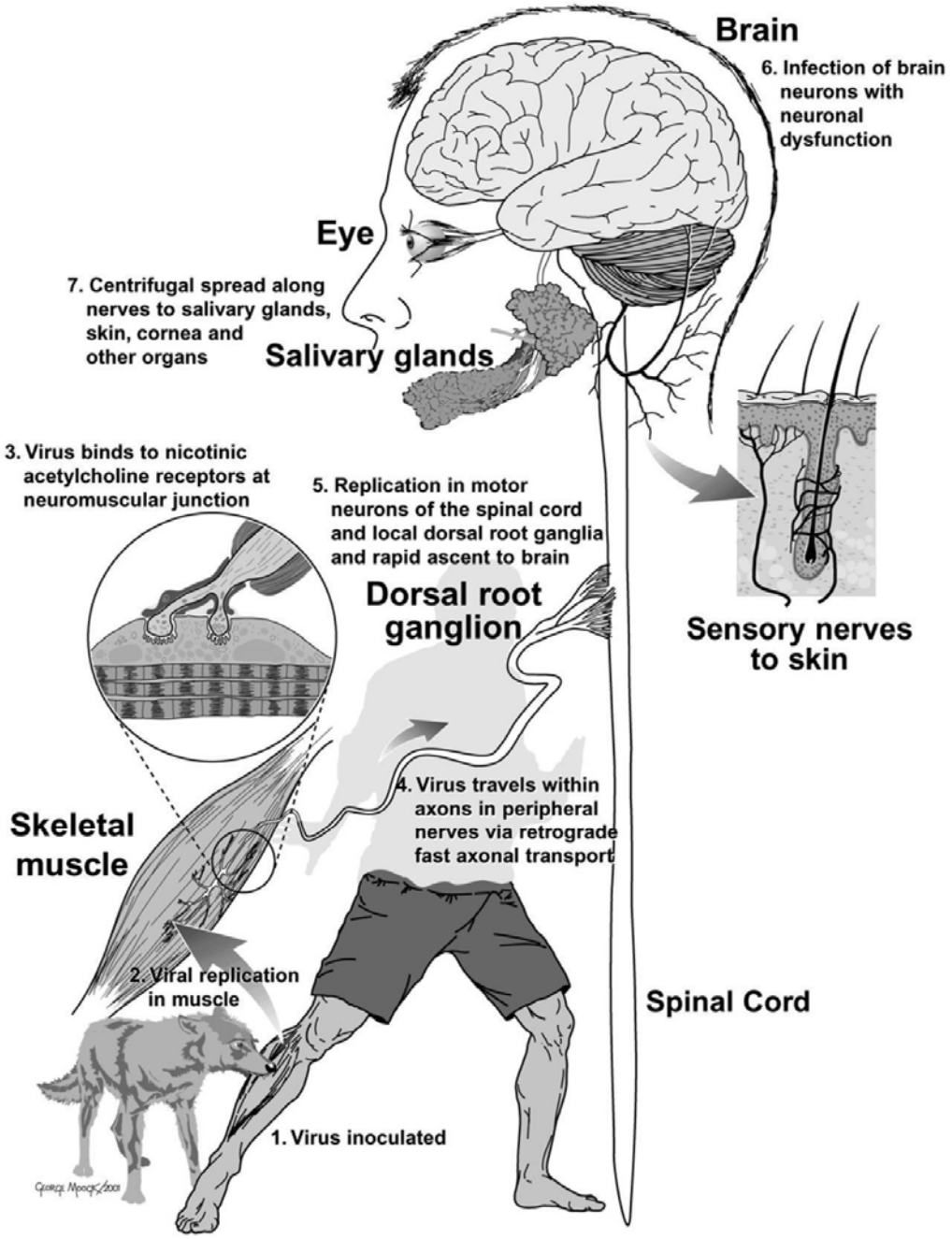

Figure 2. Schematic diagram showing the sequential steps in the pathogenesis of rabies after an animal bite (Jackson AC, 2008).

Clinical Manifestations

During the acute neurological phase, clinical features in human rabies can be distinguished as classic (encephalitic or furious and paralytic or dumb) and non-classic or atypical forms. Almost a universally fatal outcome is

expected once symptoms and signs develop. Human patients associated with dog variants exhibited more unique clinical manifestations than those with bats in the form of furious and paralytic rabies.

Different anatomical involvement of the nervous system has been shown in the case of furious and paralytic rabies. Brainstem, thalamus, basal ganglia and spinal cord are preferential sites of rabies viral infection in both forms during the early stage of illness. Access of the virus to the CNS does not necessarily lead to rapid development of symptoms and death. Furious rabies patient remains alert until the pre-terminal phase and does not exhibit any demonstrable weakness of the arms and legs until the patient lapses into coma (Mitrabhakdi et al., 2005). Pattern of consciousness of paralytic rabies patient is similar with none or minimal signs of aggression and phobic spasms. Weakness of the extremities, caused by demyelin- or axonopathy, is the initial presentation in this form of rabies. During pre-terminal or comatose phase, these 2 different forms are indistinguishable.

Neuronal dysfunction and death

Rabies is characterized by severe neurologic signs with relatively mild neuropathologic lesions. Mechanisms of neuronal dysfunctions that occur in natural rabies are still not understood.

Effects on ion channels

RV infection might have effects on transmembrane ion channel activity. RC-HL strain infected cultured mouse neuroblastoma cells show a reduction in functional expression of both voltage-dependent Na^+ channels and inward rectifier K^+ channels without changing that of delayed rectifier K^+ channel by using the whole-cell patch clamp technique (Iwata et al, 1999). Another study in NG108-15 cells, RC-HL strain infection does not found to alter the

functional expression of voltage-dependent Ca^{2+} channels, but it attenuates the α2-adrenoreceptors-mediated inhibition of Ca^{2+} channel activity (Iwata et al., 2000). These results provide evidence for possible involvement of the change in membrane properties in functional impairment.

Proteomic profiling on brain homogenates in ICR mice infected with attenuated CVS-B2C or wild type silver-haired bat rabies virus found that the expression of proteins involved in ion homeostasis was altered. Upregulation of H^+ ATPase and Na^+/K^+ ATPase as well as downregulation of Ca^{2+} ATPase were discussed alter infection with SHBRV. And there was downregulation of proteins relevant to synaptic physiology, which is involved in docking and fusion of synaptic vesicles to the presynaptic membrane (Dhingra et al., 2007).

Neuronal death

Rabies virus may induce neuronal death, possibly through apoptotic mechanisms. Lack of apoptosis in the CNS has been shown to be a marker of virulence of wild type or street rabies virus to avoid immune recognition and to facilitate spreading. The street rabies virus (silver-haired bat rabies virus, SHBRV) induced only mild histological changes and little or no Terminal deoxynucleotidyl transferase-mediated dUTP-biotin nick end labeling (TUNEL) staining in the brain of ICR mice on intracerebral injection (Yan et al., 2001). Statistical analyses revealed that the number of apoptotic cells in primary neuronal cultures and mice infected with SHBRV was not significantly different from the number in uninfected neurons or sham-infected animals by either test. Despite rabies antigen was detected in almost all in the spinal cord, little apoptosis was detected in the spinal cord or in the brain of mice infected with 10^3 ffu of SHBRV (Sarmento et al., 2005). In paraffin-embedded brain tissues of 12 cases postmortem human rabies did not demonstrate morphological features of neuronal apoptosis and TUNEL staining. Similarly, immunostained activated caspase-3 was not seen in neurons, but prominently

stained the processes of microglia (Jackson et al., 2008). The ability of the street rabies virus to activate apoptosis in nerve cells was studied in 10 brains of adult dogs by determining the DNA fragmentation and TUNEL technique. The result did not undergo apoptosis in these experiments (Suja et al., 2009).

On the contrary, fixed viruses induced marked degree of apoptosis of infected neurons. CVS strain has been observed to induce apoptotic cell death in rat prostatic adenocarcinoma (AT3) cells (Jackson and Rossiter, 1997). Characteristic morphologic features of apoptosis and evidence of oligonucleosomal DNA fragmentation was demonstrated by TUNEL staining. Higher expression of the Bax protein was decreased. Whereas, CVS-infected Bcl-2-transfected AT3 cells did not demonstrate these features. In primary culture of mouse cortical and hippocampus neurons showed that expression of activated caspase 3 and TUNEL positive staining was observed in CVS-infected neurons by 24 h p.i. and later increased (Weli et al., 2006). The experimental in CVS-11 rabies virus-infected mouse neuroblastoma cells underwent chromatin condensation (DAPI staining) and DNA fragmentation within 48 h post-infection, more evident at 72 h. An increased level of Bax, the apoptotic enhancer, was detected within 24 h after infection. In contrast, Bcl-2, the apoptotic antagonist, remained unchanged. Shortly after detection of Bax, caspase 1 (ICE) was upregulated. And after that, poly ADP-ribose polymerase (PARP) (the DNA repair enzyme) was significantly degraded (Ubol et al., 1998).

For the attenuated strain Evelyn Rotnycki Abelseth (ERA) also infects nonneuronal cells. In these reports, both rabies virus strains (CVS and ERA) infect activated murine lymphocytes and the human lymphoblastoid Jurkat T-cell line. In contrast to that of the CVS strain, ERA viral replication, is concomitant with viral glycoprotein expression, induces apoptosis of infected Jurkat T cells that demonstrated increased in cell mortality by flow cytometry, TUNEL positive and DNA electrophoresis fragmentation (Thoulouze et al.,

1997). Unlike pathogenic CVS strain, attenuated ERA strain triggers Annexin V staining. Furthermore, they observed the induction of TUNEL staining of the human lymphoblastoid cell line Jurkat rtTA (Préhaud et al., 2003). ERA-infection induce not only caspase-dependent apoptosis (pro-caspases-3, -8, and -9) in the human lymphoblastoid Jurkat T cell line (Jurkat-vect), but also a caspase-independent pathway involving the apoptosis-inducing factor (AIF). Caspase activation was detected in a higher proportion of cells infected with ERA (20 to 55% of cultured cells) than of CVS-infected cells (7 to 18% of cultured cells). AIF translocation immunostaining was induced in cultures but does not occur in all apoptotic cells (Thoulouze et al., 2003). In BSR cells infected with CVS-B2C, TUNEL staining showed that many apoptotic cells were detected in cells. For caspase activity assays, infection with CVS-B2C caused a 24% increase in total caspase activities over the negative controls infection with CVS-B2C resulted in a 14% and a 21% increase in caspase-3 and -8 activities, respectively. Caspase-9 activity increased only 4.4% indicating that the induction of apoptosis by CVS-B2C may involve an extrinsic apoptotic pathway. The 85 kDa cleaved fragment of PARP was detected. In addition, AIF was upregulated and translocated from the cytosol to the nucleus. Therefore, these results suggest that CVS-B2C induces apoptosis through caspase-dependent and caspase-independent pathways (Sarmento et al., 2005).

In animal models, prominent apoptotic death of neurons has been observed in the brains of mice of various ages inoculated intracerebrally with the CVS strain of fixed RV. 6-week-old ICR mice inoculated intracerebrally with CVS (7 days) LM shown a typical apoptotic morphology, EM Multiple condensations of nuclear chromatin cytoplasmic shrinkage most marked changes in cortical neurons and in pyramidal neurons of the hippocampus, TUNEL prominent in pyramidal neurons of the hippocampus and in cortical neurons less in the cerebellum (despite strong immunostaining for rabies virus

antigen), Immunostaining for the Bax protein (+) in pyramidal neurons of the hippocampus and cortical neurons (Weli et al., 2006; Jackson and Park, 1999).

Intriguingly, neurons of different regions display diverse degree of resistance to cell death process. It has been demonstrated that motoneurons of spinal cord, despite the massive infection, resist to apoptosis and cytolysis and remained functioning over a period of 7 days after CVS infection, whereas 70% of infected hippocampal neurons became apoptotic and died within 3 days. Moreover, axons of rabies infected motoneuron were elongated indicating that metabolic activity was maintained in these infected cells. In contrast, hippocampus neurons were apoptotic shortly after infection (Guigoni and Coulon, 2002). The reasons for these site-specific differences are not clear. Therefore, even neurons from the same region of the brain can respond in different ways to virus infection. This may reflect an inherent heterogeneity in the motor neuron population or differential virus exposure. Based on the results reported here, it may be assumed that different populations of neurons, especially in spinal cord motor neurons, respond by the different mechanism when exposed to the stimulus.

Midline CNS structures, thalamus, brainstem, basal ganglia, and spinal cord have been shown to be preferentially infected in rabies infected patients and dogs (Laothamatas, 2003, 2008, Tirawatnpong, 1989). Therefore, survival of neurons may not be depending solely on the nature of the viral stain. Differential site-specific responses may also play role. Cytochrome c leakage in the cytoplasm representing early stage of mitochondrial cell death has been demonstrated in degree of order from cortices of the brain, brainstem and spinal cord of 10 rabies pateints. Spinal cord and brainstem are heavily infected as compared to the higher levels (Juntrakul et al., 2005).

Neurotoxicity

Nitric oxide (NO) generated by Nitric oxide synthase (NOS). Different types of NO-producting enzymes have been found in the CNS. There are three known isoforms, two are constitutive (cNOS): Endothelial NOS (eNOS) and Neuronal NOS (nNOS) and the third is inducible (iNOS). During CVS-infected rats, the activity of cNOS significantly decreased without a neuronal loss (Akaike et al., 1995). Increased expression of eNOS was detected in neuron of cattle brain with natural rabies infection. Moreover, these studies demonstrated that the co-localization of eNOS and rabies neucleoprotein in inclusion bodies (Negri bodies). The result suggest that eNOS is involved in the formation of rabies inclusion bodies (Shin et al., 2004). The level of NO was determined directly in the CNS of rats infected with rabies virus. Using spin trapping of NO and electron paramagnetic resonance spectroscopy, the result show that amounts of NO (up to 30-fold more than controls) are elaborated and correlated with the onset of clinical signs and the clinical progression of disease (Hooper et al., 1995). Upregulation of the iNOS gene has been observed in rat brain that was experimentally infected with rabies virus (Van Dam, 1995). The level of iNOS mRNA expression appear to correlate with clinical severity, inflammatory, innate immunity and antioxidant (Koprowski, 1993, Shin, 2004). These results suggest that iNOS-derived NO could play an important role in the CNS damage associated with the disease states. In addition, iNOS inhibition, treatment of rabies virus-infected mice with iNOS inhibitor (aminoguanidine), delayed apoptotic deaths by affecting viral replication that may show in NO suppress RNA synthesis (N, G, L genes) (Ubol, 2001a, 2001b). In contrast, iNOS induction is essential for permiabilizing the blood-brain barrier and allowing entry of the necessary effector cells to clear the virus (Fabis, 2008). Oxidative stress has been reported in rabies. Axonal swellings with 4-HNE-labeled puncta were also associated with aggregations of actively respiring mitochondria. Jackson and his colleagues have found evidence that rabies virus infection in cultured adult mouse DRG neurons causes axonal injury through

oxidative stress (Jackson, 2010). Oxidative stress may be important in *vivo* in rabies and may explain previous observations of the degeneration of neuronal processes in studies of transgenic mice (Scott, 2008). Antioxidant proteins were found increased, more in paralytic.

CHAPTER III
MATERIALS AND METHODS

A diagram of the experimental design to determine and analyze in the expression of protein(s) in brain, brainstem and spinal cord of naturally rabies infected and non-rabies infected dogs was presented in figure 3.

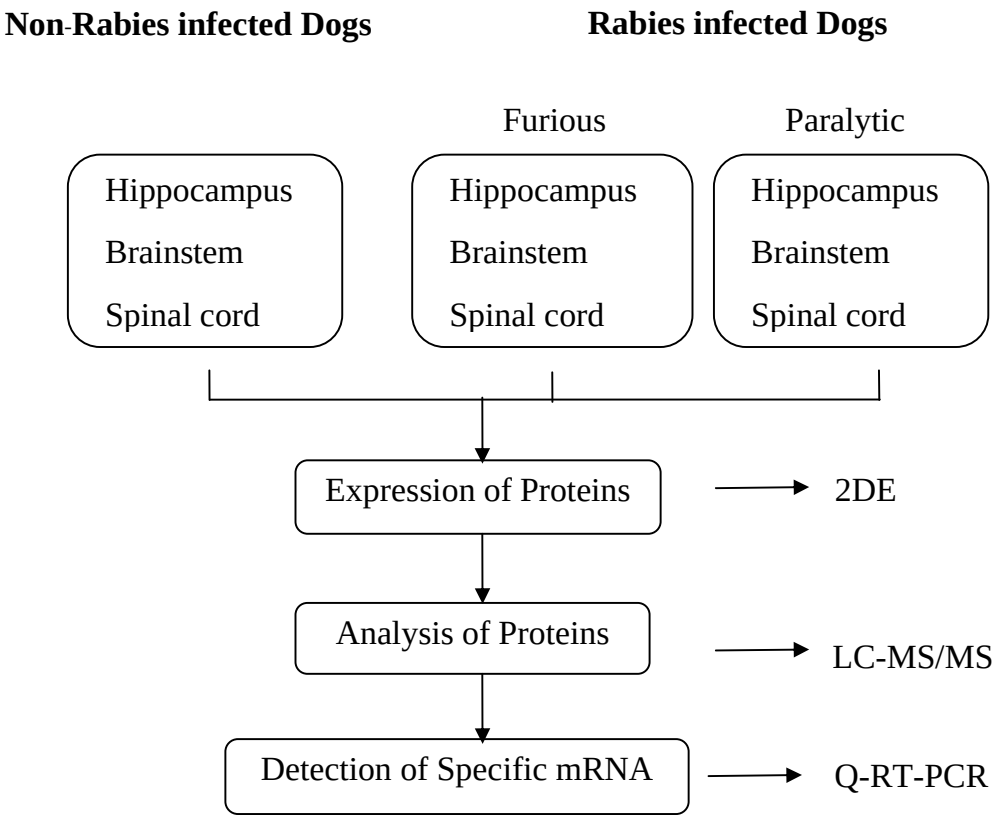

Figure 3. Diagram of the experimental designs.

Sample collection

Samples for examination and analyses were taken from rabies infected paralytic, furious, and non-infected dogs. Each animal was observed at the Quarantine and Rabies Diagnostic Unit of the Queen Saovabha Memorial Institute (QSMI). As previously described (Tirawatnpong et al., 1989; Laothamatas et al., 2008), stages of infection were clinically defined as early or late, based on whether the dogs remained fully conscious (early) or lapsed into coma (late). Further, the stage of disease was confirmed by the relative absence of rabies antigen at the cerebral hemisphere, in particular the frontal lobe. Paralytic rabies was defined by the presence of hind limb weakness with minimal or none at all of furious symptoms. This study focused on only late stage of infection. The animals died naturally without receiving any supportive treatment. From each animal, 3 anatomical locations of the CNS tissues, including hippocampus, brainstem (midbrain, pons and medulla) and cervical enlargement of spinal cord were taken and were saved at -70°C until used.

Immunoperoxidase staining of rabies antigen

The diagnosis of rabies was confirmed by the presence of rabies antigen in the CNS tissues. Paraffin-embedded sections of formalin-fixed tissues (3-µm-thick) were stained with anti-rabies nucleocapsid polyclonal antibody (Bio-Rad; Marnes-la-Coquette, France) at a dilution of 1:80. After rinsing with PBS, the sections were incubated with respective secondary antibody conjugated with horseradish peroxidase in the DAKO EnVision™-System kit (DAKO Corporation; CA) for 30 min. The slides were then washed with PBS and incubated for 10 min with a peroxidase substrate containing 0.5 mg/ml diaminobenzidine (Sigma; St. Louis, MO), 30% H_2O_2 and 1 M imidazole in Tris-

HCl buffer. After rinsing by tap water, the tissues were counterstained with hematoxylin.

Sample extraction for proteomic analysis

The sample tissues (hippocampus, brainstem and spinal cord) were frozen in liquid nitrogen and ground to powder using prechilled mortar and pestle. Tissues were resuspended in a lysis buffer containing 7 M urea, 2 M thiourea, 4% 3-[(3-cholamidopropyl) dimethyl-ammonio]-1-propanesulfonate (CHAPS), 2% v/v ampholytes (pH 3–10), 120 mM dithiothreitol (DTT), and 40mM Tris-base, and incubated at 4°C for 30 min. Unsolubilized nuclei, cell debris, and particulate matters were removed by a centrifugation at 10,000 rpm, 4°C for 5 min. Protein concentration in individual samples was measured by by the Bradford method (Bradford, 1976) using Bio-Rad protein assay (Bio-Rad Laboratories; Hercules, CA). Proteins derived from one region of each animal were further resolved in individual 2-D gels.

Two-Dimensional Gel Electrophoresis (2-DE)

For the controlled group, each gel was derived from each sample (n = 6 gels/region). For the paralytic and furious groups, duplicated 2-D gels were derived from each sample to have 6 gels/region in each group. Overall, a total of 54 gels were analyzed in this experiment.Briefly described, an equal amount of total protein from each sample was resolved in each 2-D gel (n = 6 gels in each group; total n = 54 gels). Immobiline DryStrip (non linear pH gradient of 3-10, 7 cm long; GE Healthcare, Uppsala, Sweden) was rehydrated overnight with 150 µg of total protein that was premixed with a rehydration buffer containing 7 M urea, 2 M thiourea, 2% CHAPS, 2% (v/v) ampholytes (pH 3-10), 120 mM DTT, 40 mM Tris-base, and bromophenol blue (to make the final volume of 150 µL per strip).

The first dimensional separation or isoelectric focusing (IEF) was performed in Ettan IPGphor III System (GE Healthcare) at 20°C, using a stepwise mode to reach 9,083 Vh with limiting current of 50 mA/ strip. After completion of the IEF, the strips were first equilibrated for 15 min in an equilibration buffer containing 6 M urea, 130 mM DTT, 112 mM Tris-base, 4% SDS, 30% glycerol and 0.002% bromophenol blue, and then in another similar buffer that replaced DTT with 135 mM iodoacetamide, for further 15 min. The second dimensional separation was performed in 12% polyacrylamide gel using SE260 Mini-Vertical Electrophoresis Unit (GE Healthcare) at 150V for approximately 2 h.

SYPRO Ruby staining and visualization

After 2-DE, separated proteins in slab gels were fixed with 10% methanol and 7% acetic acid for 30 min. The SYPRO Ruby fluorescence dye (Invitrogen/Molecular Probes; Eugene, OR) was added to each gel and incubated on a gentle continuous rocker in a dark room at room temperature for overnight and then visualized using Typhoon 9200 laser scanner (GE Healthcare).

Matching and Analysis of Visualized Protein Spots

Image Master 2D Platinum software (GE Healthcare) was used for matching and analysis of protein spots in 2-D gels. Parameters used for spot detection were (i) minimal area = 10 pixels; (ii) smooth factor = 2.0; and (iii) saliency = 2.0. A reference gel was created from an artificial gel combining all of the spots presenting in different gels into one image. The reference gel was then used for determination of existence and difference of protein expression between gels. Background subtraction was performed and the intensity volume of each spot was normalized with total intensity volume (summation of the intensity volumes obtained from all spots within the same 2-D gel).

Statistical analysis

All the quantitative data are reported as mean ± SEM. Intensity volumes of individual spots matched across different gels were compared among groups by multiple comparisons using one-way analysis of variance (ANOVA) with Tukey's post-hoc test (SPSS; version 13.0). P values less than 0.05 were considered as statistical significant. Significantly differed protein spots were subjected to in-gel tryptic digestion and identification by mass spectrometry.

In-gel tryptic digestion

All the protein spots whose intensity levels significantly differed among groups were excised from 2-D gels, washed twice with 200 μl of 50% acetonitrile (ACN)/25 mM NH_4HCO_3 buffer (pH 8.0) at room temperature for 15 min, and then washed once with 200 μl of 100% ACN. After washing, the solvent was removed, and the gel pieces were dried by a SpeedVac concentrator (Savant; Holbrook, NY) and rehydrated with 10 μl of 1% (w/v) trypsin (Promega; Madison, WI) in 25 mM NH_4HCO_3. After rehydration, the gel pieces were crushed and incubated at 37°C for at least 16 h. Peptides were subsequently extracted twice with 50 μl of 50% ACN/5% trifluoroacetic acid (TFA); the extracted solutions were then combined and dried with the SpeedVac concentrator. The peptide pellets were resuspended with 10 μl of 0.1% TFA and purified using $ZipTip_{C18}$ (Millipore; Bedford, MA). The peptide solution was drawn up and down in the $ZipTip_{C18}$ ten times and then washed with 10 μl of 0.1% formic acid by drawing up and expelling the washing solution three times. The peptides were finally eluted with 5 μl of 75% ACN/0.1% formic acid.

Protein identification by Q-TOF MS and MS/MS analyses

The trypsinized samples were premixed 1:1 with the matrix solution containing 5 mg/ml α-cyano-4-hydroxycinnamic acid (CHCA) in 50% ACN, 0.1% (v/v) TFA and 2% (w/v) ammonium citrate, and deposited onto the 96-well MALDI target plate. The samples were analyzed by Q-TOF Ultima™ mass spectrometer (Micromass; Manchester, UK), which was fully automated with predefined probe motion pattern and the peak intensity threshold for switching over from MS survey scanning to MS/MS, and from one MS/MS to another. Within each sample well, parent ions that met the predefined criteria (any peak within the *m/z* 800 – 3,000 range with intensity above 10 count ± include/exclude list) were selected for CID MS/MS using argon as the collision gas and a mass dependent ± 5 V rolling collision energy until the end of the probe pattern was reached. The MS and MS/MS data were extracted and outputted as the searchable *.txt* and *.pkl* files, respectively, for independent searches using the MASCOT search engine (*http://www.matrixscience.com*), assuming that peptides were monoisotopic. Fixed modification was carbamidomethylation at cysteine residues, whereas variable modification was oxidation at methionine residues. Only one missed trypsin cleavage was allowed, and peptide mass tolerances of 100 and 50 ppm were allowed for peptide mass fingerprinting and MS/MS ions search, respectively.

RNA extraction and cDNA synthesis

Total RNA was extracted from each tissue sample. The RNeasy Lipid Tissue mini Kit (Qia-gen, Hilden, Germany) was used according to the manufacturer's instructions. Total RNA was isolated from tissues using Qiazol reagent (Invitrogen Life Technologies, Carlsbad, California, USA), DNase treatment of RNA prior to RT-PCR and was subjected to reverse transcription

using PrecisionTM reverse transcription kit (Primer design) according to the manufacturer's protocol. The samples were incubated at 65°C for 5 min, followed by a final RT inactivation step at 42°C for 60 min, and then stored at -20°C until used.

SYBR Green Real-time PCR

A real-time PCR assay was performed to assure the presence of proteins as selected from 2-DE and MALDI Q-TOF mass spectrometry using LightCycler 2.0 (Roche Applied Science, Mann-heim, Germany). These included ACNTase, CRMP-2, GFAP, Hsp70 and Orp150 transcripts using GAPDH as an endogenous control. PCR amplification was performed with QuantiTect SYBR Green PCR Kit: 2× QuantiTect SYBR Green PCR Master Mix with 0.5 μM primers, 12.5 ng cDNA, and nuclease-free water according to the manufacturer’s protocol (Qiagen, Hilden, Germany). The PCR conditions were as follows: 95°C for 15 min for pre-incubation, followed by 45 cycles of 94°C for 15 s, 55°C for 30 s, and 72°C for 30 s. Levels of cDNA were expressed as threshold cycle (CT) and the melting temp was used for analysis. To avoid genomic DNA amplification, primers used in this study were designed to span intron–exon boundaries as follows in appendix B.

CHAPTER IV
RESULTS

1. Regional distribution of rabies virus in CNS

Rabies viral antigen

We investigated changes in tissue proteomes of hippocampus, brainstem and spinal cord of paralytic and furious dogs naturally infected with rabies compared to the non-infected controls. Rabies infection was confirmed in paralytic and furious dogs by positive immunoperoxidase staining of rabies nucleocapsid protein in their CNS tissues (as illustrated in brown in Figure 4). The overall regional distribution of rabies viral antigen was roughly similar in terms of number and location to that previous report (Juntrakul et al., 2005).

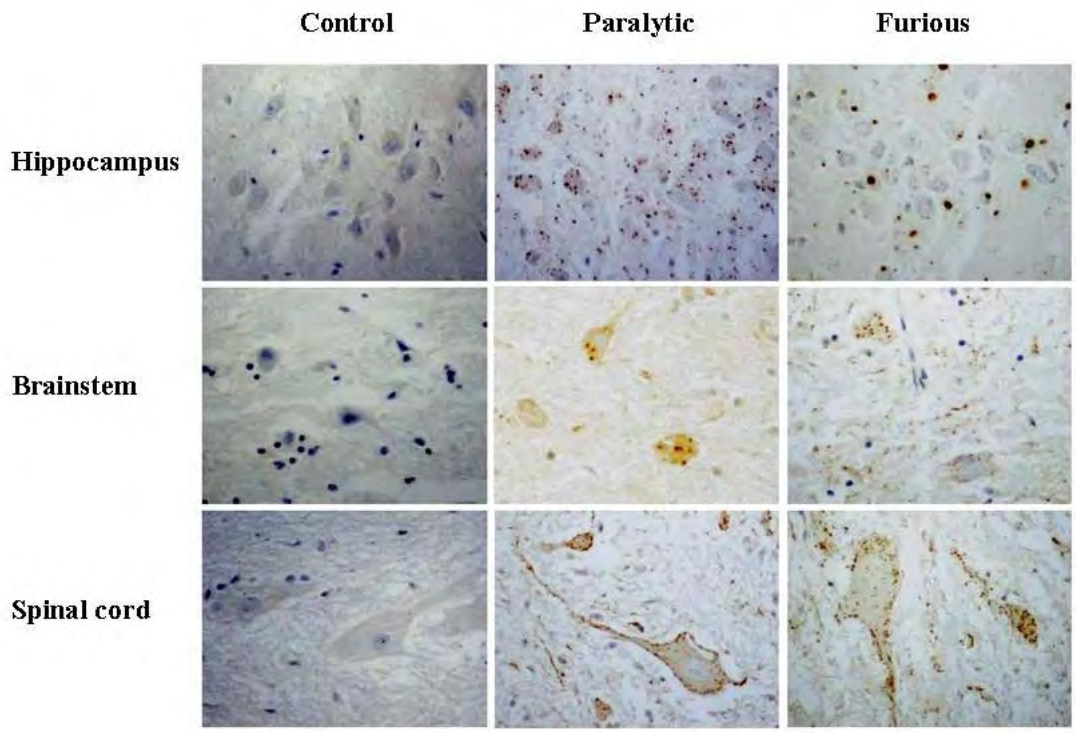

Figure 4. Immunoperoxidase staining of rabies antigen. Hippocampus, brainstem and spinal cord from non-infected dogs and those naturally infected with rabies (both paralytic and furious forms) were subjected to immunohistochemical study for rabies antigen using polyclonal antibody against rabies nucleocapsid as the primary antibody and hematoxylin as the counterstain. Immunoreactive locales of rabies nucleocapsid are shown in brown, whereas nuclei are illustrated in blue.

2. Identification of proteins with significant expression levels

2.1 2-D gels analysis

Proteins were extracted from these tissues and analyzed by 2-DE (n = 6 gels/region for each group, with or without replication of individual samples; a total of 54 gels were analyzed). From >1,000 protein spots visualized in each gel, spot matching, quantitative intensity analysis and ANOVA with Tukey's post-hoc multiple comparisons revealed 32, 49 and 67 protein spots that were differentially expressed among the three clinical groups in hippocampus (Figure 5), brainstem (Figure 6) and spinal cord (Figure 7), respectively.

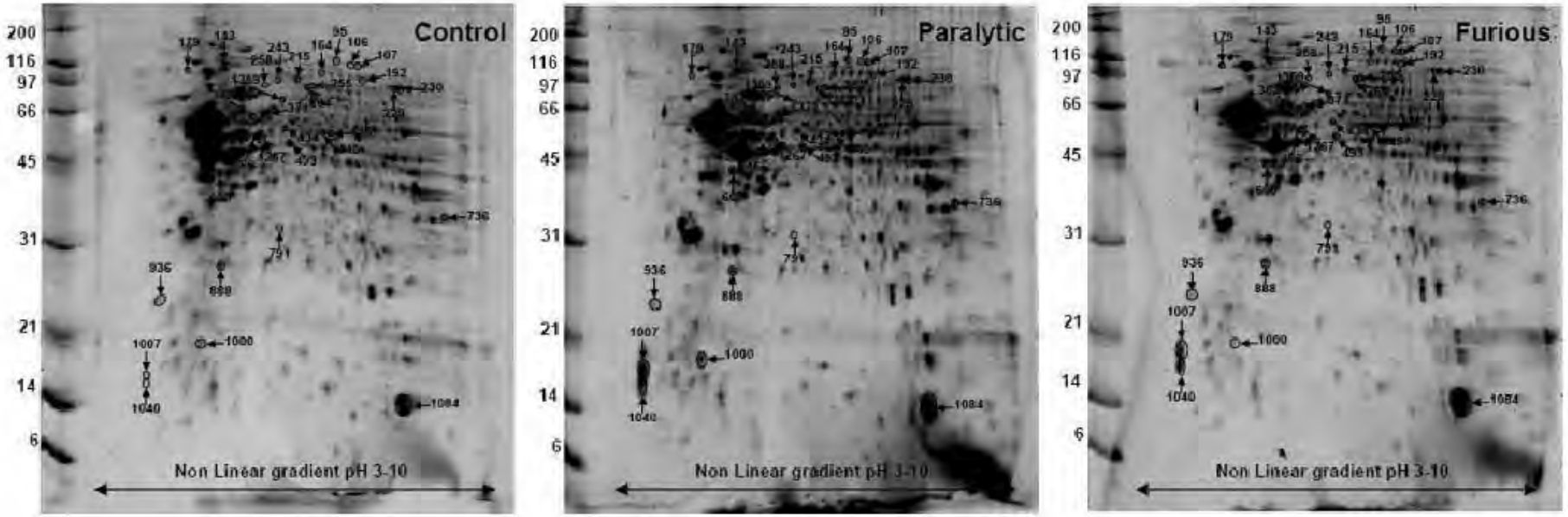

Figure 5. 2-D Proteome maps of differentially expressed proteins in hippocampus of dogs naturally infected with rabies. Proteins that significantly differed among groups, including non-infected control, paralytic form of rabies and furious form of rabies, are labeled with numbers that correspond to those reported in Tables 1.

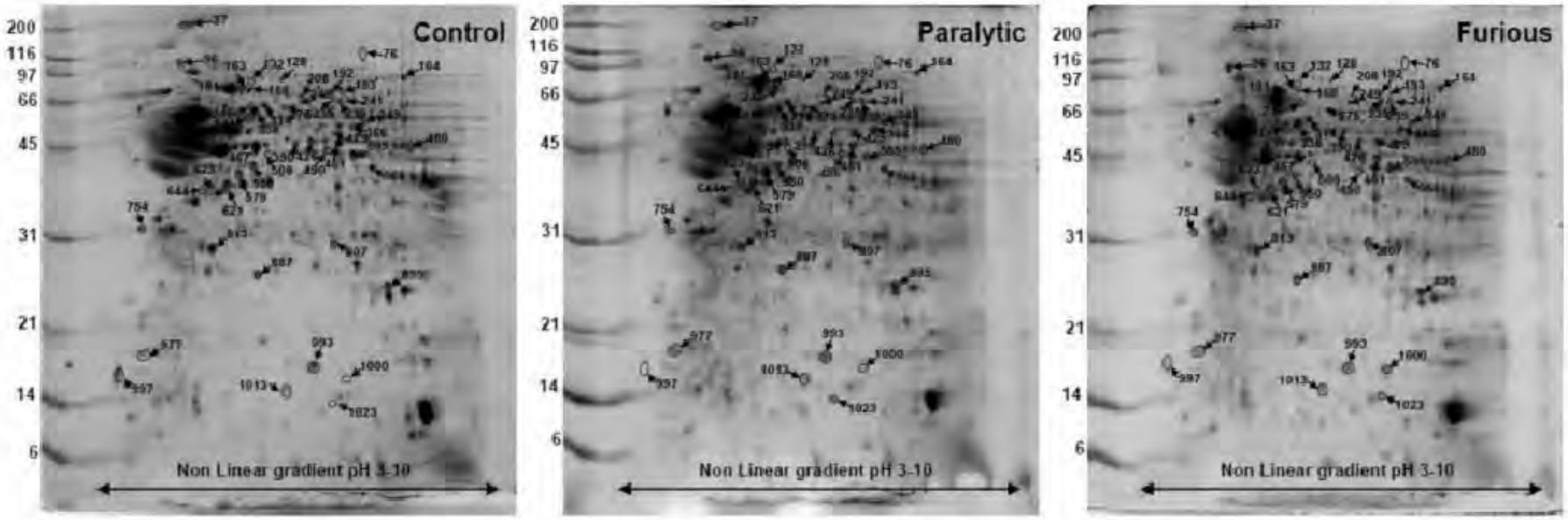

Figure 6. 2-D Proteome maps of differentially expressed proteins in brainstem of dogs naturally infected with rabies. Proteins that significantly differed among groups, including non-infected control, paralytic form of rabies and furious form of rabies, are labeled with numbers that correspond to those reported in Tables 2.

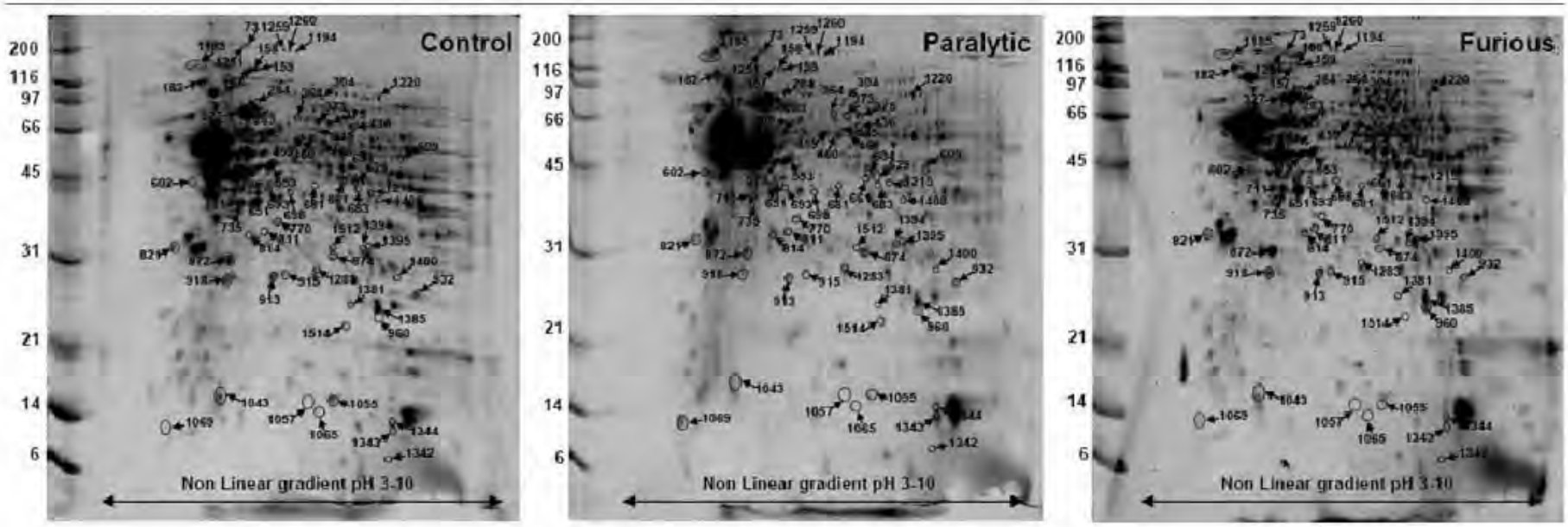

Figure 7. 2-D Proteome maps of differentially expressed proteins in spinal cord of dogs naturally infected with rabies. Proteins that significantly differed among groups, including non-infected control, paralytic form of rabies and furious form of rabies, are labeled with numbers that correspond to those reported in Tables 3.

2.2 Protein Identification by MALDI-Q-TOF MS and MS/MS Analyses

Subsequent analyses of these differentially expressed protein spots were done by MALDI Q-TOF. The criteria for the significant changes in protein abundance were defined as (i) p values must be < 0.05, (ii) means of the three groups using the multiple comparisons must have p values < 0.05.

Table 1. Summary of Altered Proteins in hippocampus region compare to non-infected (N), furious (F) and paralytic (D) groups Identified by Q-TOF MS and/or MS/MS Analyses

Spot no.	Protein name	NCBI ID	Identified by	Identification scores (MS, MS/MS)	%Cov (MS, MS/MS)	No. of matched peptides (MS, MS/MS)	p/	MW (kDa)	Intensity (Mean ± SEM)			ANOVA *p* values	Tukey's post-hoc multiple comparisons		
									Control	Paralytic	Furious		Paralytic vs Control	Furious vs Control	Paralytic vs Furious
95	Pyruvate carboxylase, mitochondrial precursor (Pyruvic carboxylase) (PCB) isoform 1	gi|73982897	MS	140, NA	21, NA	23, NA	6.32	130.25	0.0881 ± 0.0107	0.0907 ± 0.0041	0.0410 ± 0.0185	0.0225	NS	0.0456	0.0346
106	Protein C9orf55 isoform 1	gi|73971036	MS	69, NA	11, NA	18, NA	6.11	212.96	0.0696 ± 0.0106	0.0623 ± 0.0055	0.0964 ± 0.0097	0.0395	NS	NS	0.0410
107	Interferon alpha 4	gi|18767673	MS	77, NA	29, NA	6, NA	6.95	23.32	0.1034 ± 0.0076	0.1106 ± 0.0066	0.1439 ± 0.0101	0.0078	NS	0.0092	0.0313
143	Transitional endoplasmic reticulum ATPase (TER ATPase) (15S Mg(2+)-ATPase p97 subunit) (Valosin-containing protein) (VCP) isoform 13	gi|73971232	MS	79, NA	25, NA	13, NA	5.11	90.35	0.0229 ± 0.0078	0.0332 ± 0.0041	0.0521 ± 0.0059	0.0140	NS	0.0117	NS
164	Dynamin	gi|181849	MS/MS	NA, 30	1, NA	1, NA	6.93	97.75	0.1218 ± 0.0144	0.0803 ± 0.0032	0.0949 ± 0.0084	0.0288	0.0244	NS	NS
179	Propionyl-Coenzyme A carboxylase, alpha polypeptide isoform 4	gi|114650510	MS	84, NA	24, NA	14, NA	6.98	82.54	0.0376 ± 0.0120	0.0594 ± 0.0047	0.0798 ± 0.0040	0.0064	NS	0.0047	NS
192	Cytochrome P450 2B12 (CYPIIB12)	gi|62639273	MS, MS/MS	81, 27	25, 1	9, 1	8.43	56.54	0.1120 ± 0.0081	0.0798 ± 0.0014	0.1251 ± 0.0082	0.0008	0.0111	NS	0.0007
215	Mitochondrial inner membrane protein (Mitofilin) (p87/89) (Proliferation-inducing gene 4 protein) isoform 1	gi|73980353	MS	112, NA	28, NA	15, NA	6.21	83.58	0.1290 ± 0.0070	0.0825 ± 0.0033	0.0972 ± 0.0061	0.0001	0.0001	0.0036	NS
229	Aconitase 2, mitochondrial isoform 7	gi|73968976	MS	72, NA	20, NA	11, NA	8.61	85.64	0.1797 ± 0.0160	0.1297 ± 0.0054	0.1496 ± 0.0119	0.0309	0.0252	NS	NS
230	Aconitase 2, mitochondrial isoform 8	gi|73968978	MS	170, NA	32, NA	20, NA	8.07	89.05	0.3063 ± 0.0270	0.2279 ± 0.0111	0.2573 ± 0.0093	0.0218	0.0179	NS	NS
243	Unidentified								0.0189 ± 0.0084	0.0630 ± 0.0148	0.0532 ± 0.0100	0.0387	0.0398	NS	NS
255	Cytokeratin type II	gi|73996498	MS/MS	NA, 33	NA, 1	NA, 1	6.33	107.86	0.0253 ± 0.0055	0.0357 ± 0.0022	0.0173 ± 0.0056	0.0480	NS	NS	0.0390
258	Annexin A6 (Annexin VI) (Lipocortin VI) (P68) (P70) (Protein III) (Chromobindin 20) (67 kDa calelectrin) (Calphobindin-II) (CPB-II) isoform 2	gi|73953627	MS, MS/MS	109, 148	30, 8	16, 4	5.47	76.24	0.0421 ± 0.0058	0.0522 ± 0.0014	0.0578 ± 0.0031	0.0369	NS	0.0314	NS
264	Keratin 1	gi|160961491	MS, MS/MS	80, 27	25, 1	12, 1	7.62	65.62	0.0330 ± 0.0027	0.0358 ± 0.0050	0.0625 ± 0.0049	0.0004	NS	0.0007	0.0016

Table 1 (Continue)

371	Dihydropyrimidinase related protein-2 (DRP-2) (Turned on after division, 64 kDa protein) (TOAD-64) (Collapsin response mediator protein 2) (CRMP-2) isoform 3	gi|73993697	MS/MS	NA, 89	NA, 4	NA, 2	5.98	74.06	0.4072 ± 0.1000	0.2610 ± 0.0174	0.5731 ± 0.0446	0.0126	NS	NS	0.0095
382	Dihydropyrimidinase related protein-2 (DRP-2) (Turned on after division, 64 kDa protein) (TOAD-64) (Collapsin response mediator protein 2) (CRMP-2) isoform 6	gi|73993705	MS	78, NA	32, NA	12, NA	5.95	62.62	0.0834 ± 0.0375	0.1060 ± 0.0165	0.1926 ± 0.0215	0.0272	NS	0.0289	NS
434	MCG10327	gi|148690968	MS	64, NA	24, NA	8, NA	6.13	47.43	0.0545 ± 0.0121	0.0807 ± 0.0031	0.0859 ± 0.0055	0.0298	NS	0.0346	NS
445	Hypothetical protein	gi|59006605	MS	71, NA	12, NA	13, NA	8.45	149.79	0.0656 ± 0.0233	0.1267 ± 0.0092	0.1354 ± 0.0108	0.0135	0.0383	0.0178	NS
446	G patch domain containing protein 2	gi|74006169	MS	68, NA	22, NA	9, NA	9.31	59.25	0.0762 ± 0.0177	0.1243 ± 0.0072	0.1195 ± 0.0119	0.0368	0.0486	NS	NS
466	G patch domain containing protein 2	gi|74006169	MS	68, NA	22, NA	9, NA	9.31	59.25	0.4195 ± 0.0441	0.3009 ± 0.0223	0.3723 ± 0.0145	0.0402	0.0331	NS	NS
493	NADH-ubiquinone oxidoreductase 49 kDa subunit, mitochondrial precursor (Complex I-49KD) (CI-49KD) isoform 4	gi|74006142	MS	82, NA	33, NA	12, NA	7.21	51.78	0.2624 ± 0.0234	0.1804 ± 0.0169	0.1946 ± 0.0155	0.0179	0.0207	NS	NS
600	Guanine nucleotide-binding protein G(o), alpha subunit 2 isoform 1	gi|73949832	MS	71, NA	29, NA	9, NA	5.62	40.56	0.1778 ± 0.0254	0.1457 ± 0.0104	0.2802 ± 0.0271	0.0018	NS	0.0141	0.0019
736	FBXW10 protein	gi|20306882	MS	70, NA	15, NA	14, NA	9.45	122.08	0.2409 ± 0.0428	0.2500 ± 0.0288	0.1221 ± 0.0148	0.0182	NS	0.0406	0.0271
791	Hypoxanthine phosphoribosyltransferase 1	gi|50979220	MS, MS/MS	73, 30	37, 5	8, 1	5.97	24.65	0.1292 ± 0.0099	0.0947 ± 0.0126	0.0723 ± 0.0054	0.0034	NS	0.0026	NS
888	Peroxiredoxin 2 (Thioredoxin peroxidase 1) (Thioredoxin-dependent peroxide reductase 1) (Thiol-specific antioxidant protein) (TSA) (PRP) (Natural killer cell enhancing factor B) (NKEF-B) isoform 1	gi|73986497	MS	80, NA	46, NA	6, NA	5.23	22.11	0.2700 ± 0.0363	0.2982 ± 0.0272	0.4202 ± 0.0262	0.0073	NS	0.0084	0.0311

Table 1 (Continue)

936	Ryanodine receptor 2	gi|73952508	MS	78, NA	7, NA	30, NA	5.75	569.86	0.3831 ± 0.0367	0.2834 ± 0.0305	0.1647 ± 0.0443	0.0035	NS	0.0025	NS
1000	TUBB2B protein	gi|133778299	MS/MS	NA, 72	NA, 9	NA, 1	4.88	20.87	0.5454 ± 0.1100	0.4849 ± 0.0357	0.2196 ± 0.0590	0.0177	NS	0.0199	NS
1007	Keratin 1	gi|160961491	MS	81, NA	23, NA	12, NA	7.62	65.62	0.3612 ± 0.2170	1.5856 ± 0.2501	1.0169 ± 0.1782	0.0044	0.0032	NS	NS
1040	Keratin 1	gi|160961491	MS	92, NA	27, NA	13, NA	7.62	65.62	0.1234 ± 0.0991	0.5663 ± 0.1111	0.7768 ± 0.1543	0.0063	NS	0.0054	NS
1084	Beta globin	gi|57113367	MS, MS/MS	184, 140	87, 32	11, 3	7.83	16.23	3.2760 ± 0.6120	3.1782 ± 0.2172	5.6296 ± 0.0810	0.0004	NS	0.0014	0.0010
1267	Guanine deaminase	gi|73946803	MS/MS	NA, 57	NA, 2	NA, 1	6.53	63.27	0.0424 ± 0.0139	0.0456 ± 0.0102	0.1045 ± 0.0042	0.0009	NS	0.0018	0.0028
1359	SARM1 protein	gi|114325428	MS	81, NA	21, NA	12, NA	5.98	78.70	0.0231 ± 0.0118	0.0180 ± 0.0030	0.0535 ± 0.0116	0.0440	NS	0.0308	0.0204

NCBI = National Center for Biotechnology Information

%Cov = %Sequence coverage [(number of the matched residues/total number of residues in the entire sequence) x 100%]

NA = Not applicable

Table 2. Summary of Altered Proteins in brainstem region compare to non-infected (N), furious (F) and paralytic (D) groups Identified by Q-TOF MS and/or MS/MS Analyses

Spot no.	Protein name	NCBI ID	Identified by	Identification scores (MS, MS/MS)	%Cov (MS, MS/MS)	No. of matched peptides (MS, MS/MS)	p/	MW (kDa)	Intensity (Mean ± SEM)			ANOVA	Tukey's post-hoc multiple comparisons		
									Control	Paralytic	Furious	*p* values	Paralytic vs Control	Furious vs Control	Paralytic vs Furious
37	Neurofilament, heavy polypeptide 200kDa	gi|50979202	MS, MS/MS	89, 57	16, 2	16, 2	8.10	124.69	0.4792 ± 0.0901	0.0644 ± 0.0437	0.2507 ± 0.0223	0.0010	0.0048	0.0300	NS
76	Phosphatase, orphan 1 isoform 1	gi|109114246	MS	73, NA	35, NA	8, NA	7.64	30.10	0.0679 ± 0.0057	0.0253 ± 0.0093	0.0304 ± 0.0056	0.0010	0.0020	0.0055	NS
96	Heat shock protein 90kDa beta, member 1	gi|50979166	MS	72, NA	20, NA	16, NA	4.78	92.74	0.2270 ± 0.0193	0.3507 ± 0.0226	0.3002 ± 0.0205	0.0030	0.0022	NS	NS
128	Chain A, Solution Structure	gi|159164645	MS	63, NA	100, NA	5, NA	4.85	5.44	0.0365 ± 0.0077	0.0699 ± 0.0118	0.0339 ± 0.0044	0.0160	0.0363	NS	0.0241
132	Nebulin-related anchoring	gi|114632883	MS	70, NA	14, NA	19, NA	9.29	198.17	0.0632 ± 0.0069	0.0343 ± 0.0061	0.0360 ± 0.0062	0.0110	0.0174	0.0250	NS
163	Hypothetical protein LOC84070	gi|14149789	MS	74, NA	21, NA	16, NA	9.08	104.06	0.0388 ± 0.0047	0.0256 ± 0.0057	0.0169 ± 0.0038	0.0200	NS	0.0159	NS
164	Aconitase 2, mitochondrial	gi|73968980	MS, MS/MS	211, 180	37, 9	26, 5	7.89	85.87	0.1753 ± 0.0188	0.0503 ± 0.0242	0.1497 ± 0.0358	0.0130	0.0142	NS	NS
168	Mitochondrial inner membrane protein (Mitofilin) (p87/89) (Proliferation-inducing gene 4 protein) isoform 1	gi|73980353	MS, MS/MS	210, 81	40, 2	22, 2	6.21	53.58	0.0515 ± 0.0082	0.0476 ± 0.0113	0.0178 ± 0.0039	0.0240	NS	0.0317	NS
181	Unidentified								0.0764 ± 0.0085	0.0097 ± 0.0097	0.0085 ± 0.0085	0.0000	0.0003	0.0002	NS
192	Protein kinase C, gamma	gi|13384594	MS	69, NA	18, NA	12, NA	7.27	79.65	0.0424 ± 0.0031	0.0260 ± 0.0008	0.0303 ± 0.0022	0.0003	0.0003	0.0050	NS
193	Phosphofructokinase, platelet	gi|73949194	MS	112, NA	21, NA	15, NA	6.60	99.37	0.0794 ± 0.0107	0.0572 ± 0.0039	0.0512 ± 0.0042	0.0296	NS	0.0312	NS
208	Myosin, heavy chain 2,	gi|115947178	MS	72, NA	13, NA	20, NA	5.64	223.98	0.0401 ± 0.0033	0.0199 ± 0.0066	0.0313 ± 0.0034	0.0269	0.0213	NS	NS
235	N-ethylmaleimide sensitive fusion protein isoform 5	gi|73965161	MS, MS/MS	159, 88	34, 4	21, 3	6.55	83.77	0.1353 ± 0.0063	0.0949 ± 0.0032	0.1104 ± 0.0056	0.0002	0.0002	0.0108	NS
239	N-ethylmaleimide sensitive	gi|73965153	MS, MS/MS	204, 62	40, 2	26, 2	6.55	84.02	0.0830 ± 0.0064	0.0567 ± 0.0046	0.0614 ± 0.0045	0.0069	0.0081	0.0285	NS
241	N-ethylmaleimide sensitive	gi|73965159	MS, MS/MS	172, 130	32, 5	21, 4	6.55	84.98	0.0561 ± 0.0086	0.0465 ± 0.0042	0.0282 ± 0.0069	0.0345	NS	0.0297	NS
246	Annexin A6 (Annexin VI) (Lipocortin VI) (P68) (P70) (Protein III) (Chromobindin 20) (67 kDa calelectrin)	gi|73953627	MS, MS/MS	223, 41	39, 2	25, 1	5.47	76.24	0.0739 ± 0.0071	0.0722 ± 0.0074	0.0456 ± 0.0023	0.0078	NS	0.0127	0.0193

Table 2 (Continue)

249	Glutaminase, isoform CRA_a	gi|149046200	MS, MS/MS	89, 43	28, 2	12, 1	6.63	68.06	0.0481 ± 0.0023	0.0314 ± 0.0054	0.0276 ± 0.0022	0.0029	0.0150	0.0035	NS
275	Unidentified								0.0747 ± 0.0070	0.0338 ± 0.0020	0.0627 ± 0.0023	0.0000	0.0000	NS	0.0009
314	Dihydropyrimidinase related protein-2 (DRP-2) (Turned on after division, 64 kDa protein) (TOAD-64) (Collapsin response mediator protein 2) (CRMP-2) isoform 6	gi|73993705	MS, MS/MS	221, 324	51, 13	23, 5	5.95	62.62	0.1336 ± 0.0150	0.1953 ± 0.0134	0.1537 ± 0.0067	0.0087	0.0074	NS	NS
338	ATPase, H+ transporting, V1 subunit B, isoform 2 isoform 2	gi|73993820	MS,MS/MS	172, 262	50, 11	22, 4	5.65	56.14	0.3896 ± 0.0345	0.2466 ± 0.0090	0.5235 ± 0.0593	0.0008	NS	NS	0.0005
341	ATPase, H+ transporting, V1 subunit B, isoform 2 isoform 2	gi|73993820	MS, MS/MS	157, 208	48, 11	20, 4	5.65	56.14	0.2130 ± 0.0295	0.0973 ± 0.0214	0.2944 ± 0.0141	0.0001	0.0066	NS	0.0001
349	Chain A, The Crystal Structure Of Dihydrolipoamide Dehydrogenase And Dihydrolipoamide Dehydrogenase-Binding Protein (Didomain) Subcomplex Of Human Pyruvate Dehydrogenase Complex.	gi|83753870	MS, MS/MS	91, 144	38, 12	12, 4	6.50	50.66	0.1392 ± 0.0193	0.1001 ± 0.0102	0.0864 ± 0.0038	0.0279	NS	0.0270	NS
366	Fascin 1	gi|4507115	MS, MS/MS	82, 118	47, 9	17, 4	6.84	55.12	0.2224 ± 0.0232	0.1498 ± 0.0126	0.1720 ± 0.0114	0.0214	0.0191	NS	NS
390	Calcium/calmodulin-dependent protein kinase IIA isoform 1 isoform 2	gi|73953675	MS/MS	NA, 79	NA, 6	NA, 2	7.05	55.87	0.0423 ± 0.0028	0.0158 ± 0.0080	0.0276 ± 0.0114	0.0164	0.0126	NS	NS
426	Vesicle amine transport protein 1	gi|57091463	MS/MS	NA, 21	NA, 4	NA, 1	6.02	42.74	0.0993 ± 0.0047	0.0740 ± 0.0146	0.0635 ± 0.0055	0.0460	NS	0.0425	NS
429	GDP dissociation inhibitor 2	gi|50978926	MS	78, NA	31, NA	11, NA	6.11	50.80	0.1042 ± 0.0063	0.0839 ± 0.0096	0.0335 ± 0.015	0.0011	NS	0.0010	0.0135
461	Glutamine synthetase	gi|50950189	MS/MS	NA, 143	NA, 12	NA, 3	6.28	42.57	0.3038 ± 0.0181	0.2079 ± 0.0142	0.2218 ± 0.0214	0.0040	0.0053	0.0158	NS
467	Creatine kinase B-type (Creatine kinase, B chain) (B-CK) isoform 1	gi|73964131	MS	87, NA	29, NA	7, NA	5.55	44.31	0.0926 ± 0.0063	0.0419 ± 0.0089	0.0218 ± 0.0099	0.0001	0.0021	0.0001	NS
480	Phosphoglycerate kinase 1 isoform 2	gi|74007807	MSMS	NA, 101	NA, 11	NA, 3	7.99	44.89	0.2632 ± 0.0228	0.1241 ± 0.0250	0.1518 ± 0.0159	0.0009	0.0010	0.0064	NS
490	Actin-related protein 2 isoform 4	gi|73969820	MSMS	NA, 53	NA, 3	NA, 1	6.06	46.03	0.1348 ± 0.0067	0.1785 ± 0.0249	0.1128 ± 0.0063	0.0250	NS	NS	0.0216
505	Silent information regulator 2	gi|73697550	MS	93, NA	37, NA	10, NA	7.67	32.01	0.4111 ± 0.0274	0.2530 ± 0.0556	0.3516 ± 0.0160	0.0265	0.0219	NS	NS
508	Creatine kinase B-type (Creatine kinase, B chain) (B-CK) isoform 1	gi|73964131	MS, MS/MS	92, 39	45, 5	12, 2	5.55	44.31	0.0802 ± 0.0087	0.1289 ± 0.0137	0.0846 ± 0.0072	0.0076	0.0115	NS	0.0209

Table 2 (Continue)

550	GTP-binding protein alpha o	gi|8394152	MS/MS	NA, 104	NA, 9	NA, 3	5.34	40.61	0.1927 ± 0.0220	0.3018 ± 0.0375	0.1850 ± 0.0118	0.0104	0.0164	NS	0.0248
566	Silent information regulator 2	gi|73697550	MS, MS/MS	88, 22	42, 10	9, 2	7.67	32.01	0.1672 ± 0.0204	0.1711 ± 0.0177	0.0590 ± 0.0072	0.0002	NS	0.0007	0.0005
579	Tubulin, alpha 1 isoform 9	gi|73996547	MS, MS/MS	64, 126	32, 15	8, 4	4.96	46.78	0.2392 ± 0.0452	0.5260 ± 0.0861	0.2565 ± 0.0414	0.0074	0.0122	NS	0.0018
621	Guanine nucleotide-binding protein, beta-1 subunit	gi|6680045	MS, MS/MS	91, 69	41, 10	10, 3	5.60	38.15	0.3892 ± 0.0467	0.1933 ± 0.0480	0.3289 ± 0.0202	0.0111	0.0098	NS	NS
623	Tubulin alpha-2 chain (Alpha-tubulin 2) isoform 7	gi|73996522	MS, MS/MS	82, 122	23, 11	7, 3	5.00	48.86	0.1450 ± 0.0105	0.0636 ± 0.0349	0.0855 ± 0.0066	0.0441	0.0420	NS	NS
644	Unidentified								0.0842 ± 0.0163	0.0200 ± 0.0127	0.0510 ± 0.0110	0.0150	0.0114	NS	NS
754	Centrosomal protein 63kDa isoform 2	gi|194221623	MS	58, NA	37, NA	13, NA	5.69	58.31	0.1721 ± 0.0061	0.3377 ± 0.0335	0.2202 ± 0.0244	0.0007	0.0006	NS	0.0098
807	Glutathione S-transferase Mu 3 (GSTM3-3) (GST class-mu 3) (hGSTM3-3) isoform 1	gi|57088159	MS/MS	NA, 32	NA, 7	NA, 1	6.74	27.32	0.1705 ± 0.0128	0.2736 ± 0.0398	0.1591 ± 0.0229	0.0186	0.0452	NS	0.0257
813	Unidentified								0.4906 ± 0.0173	0.3973 ± 0.0308	0.5654 ± 0.0213	0.0006	0.0360	NS	0.0004
887	ATP synthase, H+ transporting, mitochondrial F0 complex, subunit d isoform a	gi|57092471	MS/MS	NA, 63	NA, 8	NA, 1	5.40	18.68	0.2529 ± 0.0077	0.3795 ± 0.0516	0.3091 ± 0.0203	0.0446	0.0360	NS	NS
895	Alpha crystallin B chain (Alpha(B)-crystallin) (Rosenthal fiber component) (Heat-shock protein beta-5) (HspB5) isoform 1	gi|57085977	MS	84, NA	56, NA	9, NA	6.76	20.05	0.3015 ± 0.0109	0.3478 ± 0.0277	0.4039 ± 0.0239	0.0170	NS	0.0130	NS
977	Unidentified								0.2259 ± 0.0148	0.5457 ± 0.0711	0.3730 ± 0.0562	0.0026	0.0018	NS	NS
993	Cytosolic purine 5-nucleotidase (5-nucleotidase cytosolic II) isoform 8	gi|73998435	MS	60, NA	20, NA	10, NA	5.88	66.25	0.3931 ± 0.0260	0.6284 ± 0.0636	0.4158 ± 0.0390	0.0041	0.0063	NS	0.0128
997	Unidentified								0.2259 ± 0.0148	0.5457 ± 0.0711	0.3730 ± 0.0562	0.0026	NS	0.0150	NS
1000	Unidentified								0.0931 ± 0.0101	0.1017 ± 0.0117	0.2252 ± 0.0550	0.0216	NS	0.0321	0.0457
1013	NAD(P) dependent steroid dehydrogenase-like isoform 1	gi|74008671	MS	51, NA	21, NA	7, NA	7.17	40.97	0.1609 ± 0.0059	0.2792 ± 0.0247	0.2659 ± 0.0149	0.0003	0.0005	0.0015	NS
1023	Immunoglobulin heavy chain variable region	gi|112700066	MS	69, NA	71, NA	6, NA	8.56	11.08	0.2323 ± 0.0192	0.4159 ± 0.0349	0.2525 ± 0.0302	0.0007	0.0012	NS	0.0031

NCBI = National Center for Biotechnology Information

%Cov = %Sequence coverage [(number of the matched residues/total number of residues in the entire sequence) x 100%]

NA = Not applicable

Table 3. Summary of Altered Proteins in spinal cord region compare to non-infected (N), furious (F) and paralytic (D) groups Identified by Q-TOF MS and/or MS/MS Analyses

Spot no.	Protein name	NCBI ID	Identified by	Identification scores (MS, MS/MS)	%Cov (MS, MS/MS)	No. of matched peptides (MS, MS/MS)	p/	MW (kDa)	Intensity (Mean ± SEM)			ANOVA *p* values	Tukey's post-hoc multiple comparisons		
									Control	Paralytic	Furious		Paralytic vs Control	Furious vs Control	Paralytic vs Furious
73	150 kDa oxygen-regulated protein precursor (Orp150) (Hypoxia up-regulated 1)	gi|73955046	MS, MS/MS	75, 76	16, 2	14, 2	5.46	122.21	0.0341 ± 0.0045	0.1260 ± 0.0264	0.0750 ± 0.0233	0.0376	0.0300	NS	NS
157	Oxygen-regulated protein 1; AltName: Full=Retinitis pigmentosa RP1 protein homolog	gi|62900882	MS	84, NA	11, NA	20, NA	5.61	242.48	0.0231 ± 0.0035	0.0000 ± 0.0000	0.0214 ± 0.0071	0.0047	0.0076	NS	0.0130
158	rCG47063	gi|149028757	MS	79, NA	21, NA	15, NA	6.82	121.89	0.0375 ± 0.0045	0.0000 ± 0.0000	0.0332 ± 0.0095	0.0010	0.0015	NS	0.0042
159	Hypothetical rhabdomyosarcoma antigen Mu-RMS-40.6c	gi|48476968	MS	76, NA	18, NA	10, NA	4.97	49.75	0.0630 ± 0.0070	0.0087 ± 0.0048	0.0411 ± 0.0100	0.0007	0.0005	NS	0.0266
182	Heat shock protein 90kDa beta, member 1	gi|50979166	MS, MS/MS	137, 87	30, 4	23, 3	4.78	92.74	0.3857 ± 0.0451	0.3422 ± 0.0475	0.1595 ± 0.0373	0.0090	NS	0.0101	0.0370
283	NADH dehydrogenase (ubiquinone) Fe-S protein 1, 75kDa precursor isoform 1	gi|57110953	MS	123, NA	32, NA	17, NA	5.85	80.65	0.0410 ± 0.0095	0.0402 ± 0.0048	0.0000 ± 0.0000	0.0005	NS	0.0011	0.0013
284	NADH dehydrogenase (ubiquinone) Fe-S protein 1, 75kDa precursor isoform 4	gi|74005206	MS	84, NA	23, NA	13, NA	6.10	81.06	0.0533 ± 0.0038	0.0318 ± 0.0099	0.0070 ± 0.0070	0.0045	NS	0.0033	NS
304	Werner helicase interacting protein 1, isoform CRA_b	gi|148700412	MS	82, NA	21, NA	10, NA	5.89	63.96	0.0527 ± 0.0031	0.0363 ± 0.0072	0.1077 ± 0.0110	0.0001	NS	0.0008	0.0001
327	Heat shock cognate 71 kDa protein (Heat shock 70 kDa protein 8)	gi|123647	MS, MS/MS	117, 148	30, 9	16, 4	5.24	70.99	0.2055 ± 0.0237	0.3348 ± 0.0182	0.2743 ± 0.0391	0.0229	0.0177	NS	NS
364	Dihydropyrimidinase related protein-2 (DRP-2) (CRMP-2) isoform 6 (Turned on after division, 64 kDa protein) (TOAD-64) (Collapsin response mediator protein 2)	gi|73993705	MS	124, NA	41, NA	17, NA	5.95	62.62	0.0295 ± 0.0094	0.0172 ± 0.0052	0.0000 ± 0.0000	0.0194	NS	0.0153	NS
373	Dihydropyrimidinase related protein-2 (DRP-2) (Turned on after division, 64 kDa protein) (TOAD-64) (Collapsin response mediator protein 2) (CRMP-2) isoform 4	gi|73993699	MS/MS	NA, 302	NA, 14	NA, 5	5.80	62.17	0.1654 ± 0.0143	0.0786 ± 0.0099	0.0947 ± 0.0226	0.0056	0.0066	0.0249	NS
375	Dihydropyrimidinase related protein-2 (DRP-2) (Turned on after division, 64 kDa protein) (TOAD-64) (Collapsin response mediator protein 2) (CRMP-2) isoform 6	gi|73993705	MS, MS/MS	226, 372	54, 15	24, 5	5.95	62.62	0.2287 ± 0.0307	0.1062 ± 0.0174	0.0925 ± 0.0058	0.0008	0.0031	0.0013	NS

Table 3 (Continue)

408	Dihydropyrimidinase-like 2	gi|40254595	MS, MS/MS	187, 293	45, 14	20, 5	5.95	62.64	0.2805 ± 0.0384	0.1761 ± 0.0329	0.3310 ± 0.0298	0.0244	NS	NS	0.0212
436	Unidentified								0.0494 ± 0.0051	0.0468 ± 0.0050	0.0092 ± 0.0060	0.0002	NS	0.0005	0.0009
445	Glial fibrillary acidic protein, astrocyte (GFAP) isoform 2	gi|73965502	MS, MS/MS	109, 23	43, 2	16, 1	5.63	49.52	0.0174 ± 0.0059	0.0371 ± 0.0069	0.0000 ± 0.0000	0.0017	NS	NS	0.0012
459	Glial fibrillary acidic protein, astrocyte (GFAP) isoform 1	gi|73965500	MS	90, NA	34, NA	13, NA	5.63	49.52	0.0620 ± 0.0050	0.0517 ± 0.0032	0.1421 ± 0.0210	0.0003	NS	0.0013	0.0004
460	Septin-8	gi|73971156	MS, MS/MS	90, 52	29, 4	13, 2	6.35	61.56	0.0907 ± 0.0047	0.0126 ± 0.0106	0.0516 ± 0.0047	0.0000	0.0000	0.0118	0.0118
469	Chaperonin containing TCP1, subunit 2 isoform 1	gi|73968673	MS	160, NA	44, NA	48, NA	6.01	57.74	0.1049 ± 0.0087	0.0837 ± 0.0081	0.1453 ± 0.0194	0.0173	NS	NS	0.0146
553	Creatine kinase B-type (Creatine kinase, B chain) (B-CK) isoform 1	gi|73964131	MS, MS/MS	236, 324	54, 18	21, 5	5.55	44.31	0.6536 ± 0.0330	0.6194 ± 0.0661	0.8821 ± 0.0517	0.0110	NS	0.0330	0.0144
579	Creatine kinase B-type (Creatine kinase, B chain) (B-CK) isoform 1	gi|73964131	MS, MS/MS	218, 242	54, 18	18, 5	5.55	44.31	0.4507 ± 0.0290	0.4179 ± 0.0323	0.6666 ± 0.0596	0.0023	NS	0.0093	0.0033
602	Glial fibrillary acidic protein, astrocyte (GFAP) isoform 1	gi|73965500	MS	135, NA	38, NA	16, NA	5.63	49.52	0.0585 ± 0.0379	0.1897 ± 0.1438	4.3635 ± 0.4024	0.0000	NS	0.0000	0.0000
609	Creatine kinase, mitochondrial 1B precursor isoform 1	gi|57108147	MS, MS/MS	87, 187	29, 14	11, 4	8.60	47.45	0.1315 ± 0.0297	0.2570 ± 0.0208	0.1459 ± 0.0425	0.0339	0.0433	NS	NS
629	Fructose-bisphosphate aldolase C (Brain-type aldolase) isoform 1	gi|57091277	MS, MS/MS	148, 220	52, 18	15, 4	6.21	39.72	0.4337 ± 0.0392	0.2344 ± 0.0208	0.3765 ± 0.0454	0.0055	0.0050	NS	0.0425
634	Fructose-bisphosphate aldolase C (Brain-type aldolase) isoform 2	gi|73966974	MS, MS/MS	56, 88	41, 13	7, 2	5.90	31.32	0.0640 ± 0.0110	0.0090 ± 0.0076	0.0703 ± 0.0200	0.0149	0.0381	NS	0.0207
651	Isocitrate dehydrogenase 3 (NAD+) alpha isoform 2	gi|73951310	MS	64, NA	36, NA	10, NA	5.86	35.09	0.1590 ± 0.0061	0.1092 ± 0.0059	0.2230 ± 0.0127	0.0000	0.0041	0.0005	0.0000
661	Silent information regulator 2	gi|73697550	MS	70, NA	41, NA	8, NA	7.67	32.01	0.1419 ± 0.0139	0.1653 ± 0.0132	0.0792 ± 0.0254	0.0167	NS	NS	0.0158
681	Keratin 1	gi|160961491	MS	90, NA	26, NA	13, NA	7.62	65.62	0.0413 ± 0.0019	0.0329 ± 0.0052	0.0145 ± 0.0073	0.0130	NS	0.0114	NS
683	Silent information regulator 2	gi|73697550	MS/MS	NA, 57	NA, 15	NA, 3	7.67	32.01	0.1611 ± 0.0288	0.0973 ± 0.0112	0.0740 ± 0.0185	0.0295	NS	0.0281	NS
693	Zinc finger protein 615	gi|197102729	MS	58, NA	24, NA	16, NA	9.31	86.12	0.1327 ± 0.0094	0.1273 ± 0.0073	0.1698 ± 0.0141	0.0316	NS	NS	0.0394

Table 3 (Continue)

698	Keratin 1	gi|160961491	MS	96, NA	26, NA	12, NA	7.62	65.62	0.1207 ± 0.0148	0.0849 ± 0.0108	0.1658 ± 0.0247	0.0222	NS	NS	0.0173
711	Chromosome 1 open reading frame 27	gi|126306536	MS	79, NA	21, NA	7, NA	6.37	53.56	0.1848 ± 0.0194	0.2134 ± 0.0278	0.3747 ± 0.0224	0.0002	NS	0.0003	0.0013
735	N-ethylmaleimide sensitive fusion protein attachment protein beta	gi|62645998	MS	87, NA	41, NA	11, NA	5.88	40.32	0.0988 ± 0.0099	0.1470 ± 0.0457	0.0000 ± 0.0000	0.0155	NS	NS	0.0134
770	3-hydroxyisobutyrate dehydrogenase, mitochondrial precursor (HIBADH) isoform 1	gi|73976179	MS	89, NA	24, NA	8, NA	8.38	35.68	0.1274 ± 0.0039	0.0685 ± 0.0118	0.0855 ± 0.0071	0.0014	0.0013	0.0166	NS
811	Myotubularin related protein 6	gi|194672062	MS	76, NA	27, NA	12, NA	7.29	71.00	0.1762 ± 0.0133	0.0835 ± 0.0066	0.1628 ± 0.0140	0.0001	0.0002	NS	0.0009
814	Cytoplasmic beta-actin isoform 2	gi|73958067	MS/MS	NA, 71	NA, 7	NA, 2	5.29	42.08	0.0935 ± 0.0197	0.1495 ± 0.0279	0.0139 ± 0.0139	0.0037	NS	NS	0.0028
821	Complement component 1, q subcomponent binding protein precursor	gi|73955331	MS/MS	NA, 27	NA, 5	NA, 1	4.77	30.42	0.3736 ± 0.0209	0.2669 ± 0.0160	0.4236 ± 0.0577	0.0270	NS	NS	0.0238
872	Ubiquitin carboxy-terminal hydrolase L1	gi|73951868	MS/MS	NA, 126	NA, 11	NA, 2	5.95	35.32	0.5050 ± 0.0347	0.3185 ± 0.0398	0.5122 ± 0.0482	0.0105	0.0226	NS	0.0180
874	Heat shock protein beta-1	gi|50979116	MS, MS/MS	74, 96	31, 12	8, 2	6.23	22.93	0.3965 ± 0.0214	0.3070 ± 0.0141	0.6276 ± 0.0376	0.0000	NS	0.0001	0.0000
913	ATP synthase, H+ transporting, mitochondrial F0 complex, subunit d isoform a	gi|57108097	MS, MS/MS	53, 99	77, 26	11, 3	5.64	18.70	0.3123 ± 0.0156	0.2056 ± 0.0114	0.2918 ± 0.0095	0.0001	0.0001	NS	0.0009
915	DJ-1 protein isoform 1	gi|57086915	MS/MS	NA, 31	NA, 7	NA, 1	5.97	20.17	0.2451 ± 0.0189	0.1234 ± 0.0055	0.1872 ± 0.0267	0.0018	0.0012	NS	NS
918	Peroxiredoxin 2 (Thioredoxin peroxidase 1) (Thioredoxin-dependent peroxide reductase 1) (Thiol-specific antioxidant protein) (TSA) (PRP) (Natural killer cell enhancing factor B) (NKEF-B) isoform 1	gi|73986497	MS/MS	NA, 169	NA, 23	NA, 4	5.20	22.11	0.3579 ± 0.0243	0.2140 ± 0.0242	0.4055 ± 0.046	0.0035	0.0247	NS	0.0035
932	Peroxiredoxin 1	gi|4505591	MS, MSMS	113, 46	44, 10	11, 2	8.27	22.32	0.2288 ± 0.0154	0.1288 ± 0.0148	0.1712 ± 0.0128	0.0013	0.0010	0.0452	NS
960	Alpha-crystallin B chain (Alpha(B)-crystallin)	gi|149716488	MS	85, NA	48, NA	8, NA	6.76	19.98	0.5524 ± 0.0525	0.2190 ± 0.0289	0.7896 ± 0.0898	0.0001	0.0054	0.0452	0.0000
1043	Fatty acid-binding protein, brain (B-FABP) (Brain lipid-binding protein) (BLBP) (Mammary derived growth inhibitor related)	gi|73946307	MS, MS/MS	68, 182	70, 27	10, 3	5.19	15.04	0.4825 ± 0.1061	0.1939 ± 0.0361	0.2126 ± 0.0537	0.0231	0.0342	0.0484	NS
1055	DnaJ (Hsp40) homolog, subfamily C, member 15 (predicted), isoform CRA_b	gi|149050007	MS	66, NA	66, NA	5, NA	10.21	6.43	0.3574 ± 0.0272	0.1871 ± 0.0092	0.2475 ± 0.0125	0.0000	0.0000	0.0020	NS
1057	Alpha-S1-casein	gi|162794	MS/MS	NA, 115	NA, 11	NA, 2	4.85	24.54	0.1663 ± 0.0543	0.0285 ± 0.0185	0.0000 ± 0.0000	0.0075	0.0291	0.0089	NS

Table 3 (Continue)

1065	Dihydrouridine synthase 1-like (S. cerevisiae)	gi|123288584	MS	71, NA	21, NA	10, NA	8.85	55.29	0.1881 ± 0.0199	0.1801 ± 0.0299	0.2720 ± 0.012	0.0329	NS	NS	0.0449
1069	S-100 calcium-binding protein beta subunit (S-100 protein, beta chain)	gi|74001608	MS/MS	NA, 40	NA, 3	NA, 1	9.91	49.49	0.7950 ± 0.0532	0.3898 ± 0.0235	0.2685 ± 0.0367	0.0000	0.0000	0.0000	NS
1185	NEFM protein	gi|148342538	MS	91, NA	21, NA	15, NA	4.85	98.39	0.2874 ± 0.0160	0.1145 ± 0.0387	0.3737 ± 0.0517	0.0015	0.0394	0.0245	NS
1194	Pyruvate carboxylase, mitochondrial precursor (Pyruvic carboxylase) (PCB) isoform 1	gi|73982897	MS, MS/MS	212, 22	28, 1	27, 1	6.32	130.25	0.0225 ± 0.0132	0.1121 ± 0.0233	0.0613 ± 0.0091	0.0127	0.0098	NS	NS
1215	Annexin A2	gi|18645167	MS	70, NA	38, NA	10, NA	7.57	38.78	0.1893 ± 0.0276	0.1379 ± 0.0182	0.0868 ± 0.0191	0.0227	NS	0.0175	NS
1220	Serotransferrin precursor (Transferrin) (Siderophilin) (Beta-1-metal binding globulin) isoform 1	gi|73990142	MS, MS/MS	239, 186	42, 8	27, 5	7.73	80.22	0.0647 ± 0.0102	0.1730 ± 0.0231	0.0849 ± 0.0173	0.0033	0.0039	NS	0.0166
1251	Collagen, type VI, alpha 1 isoform 1	gi|119887130	MS/MS	NA, 73	NA, 3	NA, 3	5.24	109.74	0.0041 ± 0.0041	0.0881 ± 0.0190	0.0050 ± 0.0050	0.0006	0.0014	NS	0.0016
1259	Vinculin (Metavinculin)	gi|73953587	MS	88, NA	22, NA	16, NA	6.82	87.67	0.0000 ± 0.0000	0.1152 ± 0.0246	0.0691 ± 0.0111	0.0015	0.0011	0.0404	NS
1260	Xin actin-binding repeat containing 2 isoform 1	gi|66841385	MS	79, NA	9, NA	30, NA	5.83	431.30	0.0165 ± 0.0110	0.1183 ± 0.0278	0.0669 ± 0.0106	0.0132	0.0099	NS	NS
1283	Thymopoietin II	gi|229542	MS	78, NA	97, NA	5, NA	8.04	55.59	0.0000 ± 0.0000	0.1248 ± 0.0057	0.1722 ± 0.0153	0.0000	0.0000	0.0000	0.0091
1342	Hypothetical protein	gi|6808049	MS	62, NA	95, NA	6, NA	4.68	5.07	0.0000 ± 0.0000	0.1968 ± 0.0408	0.0791 ± 0.0520	0.0134	0.0105	NS	NS
1343	Beta globin	gi|57113367	MS, MS/MS	181, 211	87, 42	11, 5	7.83	16.23	0.1932 ± 0.0802	0.8061 ± 0.1392	0.3819 ± 0.1471	0.0176	0.0157	NS	NS
1344	Beta globin	gi|57113367	MS, MS/MS	133, 61	86, 8	10, 1	7.83	16.23	0.0000 ± 0.0000	0.4206 ± 0.0366	0.2362 ± 0.0817	0.0002	0.0002	0.0180	NS
1381	Keratin 10 isoform 2	gi|114667513	MS	90, NA	29, NA	13, NA	5.05	56.86	0.0176 ± 0.0176	0.0756 ± 0.0227	0.3540 ± 0.1066	0.0047	NS	0.0057	0.0205
1385	Alpha crystallin B chain (Alpha(B)-crystallin) (Rosenthal fiber component) (Heat-shock protein beta-5) (HspB5) isoform 1	gi|57085977	MS, MS/MS	120, 187	60, 26	11, 3	6.76	20.05	0.0076 ± 0.0076	0.4507 ± 0.0203	0.1978 ± 0.0448	0.0000	0.0000	0.0011	0.0001
1394	40S ribosomal protein S3a (V-fos transformation effector protein) isoform 11	gi|73977917	MS	58, NA	25, NA	6, NA	9.93	30.69	0.1508 ± 0.0410	0.0887 ± 0.0187	0.2208 ± 0.0126	0.0152	NS	NS	0.0116
1395	Carbonic anhydrase I (Carbonate dehydratase I) (CA-I) (Carbonic anhydrase B)	gi|57108007	MS, MS/MS	120, 71	60, 5	11, 1	6.59	29.03	0.1720 ± 0.0571	0.1475 ± 0.0069	0.0000 ± 0.0000	0.0048	NS	0.0063	0.0178

Table 3 (Continue)

1400	Flavin reductase (FR) (NADPH-dependent diaphorase) (NADPH-flavin reductase) (FLR) (Biliverdin reductase B) (BVR-B) (Biliverdin-IX beta-reductase) (Green heme binding protein) (GHBP)	gi|73948324	MS, MS/MS	78, 33	48, 7	6, 1	7.12	22.24	0.0262 ± 0.0128	0.0947 ± 0.0192	0.0395 ± 0.0177	0.0417	0.0450	NS	NS
1408	Annexin A2	gi|50950177	MS, MS/MS	200, 175	58, 14	18, 3	6.92	38.92	0.1237 ± 0.0270	0.3673 ± 0.0710	0.2773 ± 0.0429	0.0258	0.0214	NS	NS
1512	Heat shock protein beta-1	gi|50979116	MS/MS	NA, 99	NA, 12	NA, 2	6.23	22.93	0.0000 ± 0.0000	0.1178 ± 0.0105	0.0191 ± 0.0191	0.0000	0.0000	NS	0.0003
1514	Glycogen phosphorylase, muscle form (Myophosphorylase)	gi|1730556	MS	76, NA	19, NA	16, NA	6.91	97.73	0.0906 ± 0.0323	0.0644 ± 0.0049	0.1619 ± 0.0258	0.0319	NS	NS	0.0304

NCBI = National Center for Biotechnology Information

%Cov = %Sequence coverage [(number of the matched residues/total number of residues in the entire sequence) x 100%]

NA = Not applicable

Table 4: Summary of significant differences between furious and paralytic rabies.

	Protein name	NCBI ID	Spot no.	Intensity (Mean ± SEM)			ANOVA *p* value	Multiple comparisons		
				Control [C]	Paralytic [P]	Furious [F]		P vs. C	F vs. C	P vs. F
Hippocampus										
	Beta globin	gi|57113367	1084	3.2760 ± 0.6120	3.1782 ± 0.2172	5.6296 ± 0.0810	0.0004	NS	0.0014	0.001
	Cytochrome P450 2B12 (CYPIIB12)	gi|62639273	192	0.1120 ± 0.0081	0.0798 ± 0.0014	0.1251 ± 0.0082	0.0008	0.0111	NS	0.0007
	Cytokeratin type II	gi|73996498	255	0.0253 ± 0.0055	0.0357 ± 0.0022	0.0173 ± 0.0056	0.048	NS	NS	0.039
	Dihydropyrimidinase related protein-2 (DRP-2) (Turned on after division, 64 kDa protein) (TOAD-64) (Collapsin response mediator protein 2) (CRMP-2) isoform 3	gi|73993697	371	0.4072 ± 0.1000	0.2610 ± 0.0174	0.5731 ± 0.0446	0.0126	NS	NS	0.0095
	FBXW10 protein	gi|20306882	736	0.2409 ± 0.0428	0.2500 ± 0.0288	0.1221 ± 0.0148	0.0182	NS	0.0406	0.0271
	Guanine deaminase	gi|73946803	1267	0.0424 ± 0.0139	0.0456 ± 0.0102	0.1045 ± 0.0042	0.0009	NS	0.0018	0.0028
	Guanine nucleotide-binding protein G(o), alpha subunit 2 isoform 1	gi|73949832	600	0.1778 ± 0.0254	0.1457 ± 0.0104	0.2802 ± 0.0271	0.0018	NS	0.0141	0.0019
	Interferon alpha 4	gi|18767673	107	0.1034 ± 0.0076	0.1106 ± 0.0066	0.1439 ± 0.0101	0.0078	NS	0.0092	0.0313
	Keratin 1	gi|160961491	264	0.0330 ± 0.0027	0.0358 ± 0.0050	0.0625 ± 0.0049	0.0004	NS	0.0007	0.0016
	Peroxiredoxin 2 (Thioredoxin peroxidase 1) (Thioredoxin-dependent peroxide reductase 1) (Thiol-specific antioxidant protein) (TSA) (PRP) (Natural killer cell enhancing factor B) (NKEF-B) isoform 1	gi|73986497	888	0.2700 ± 0.0363	0.2982 ± 0.0272	0.4202 ± 0.0262	0.0073	NS	0.0084	0.0311
	Protein C9orf55 isoform 1	gi|73971036	106	0.0696 ± 0.0106	0.0623 ± 0.0055	0.0964 ± 0.0097	0.0395	NS	NS	0.041
	Pyruvate carboxylase, mitochondrial precursor (Pyruvic carboxylase) (PCB) isoform 1	gi|73982897	95	0.0881 ± 0.0107	0.0907 ± 0.0041	0.0410 ± 0.0185	0.0225	NS	0.0456	0.0346
	SARM1 protein	gi|114325428	1359	0.0231 ± 0.0118	0.0180 ± 0.0030	0.0535 ± 0.0116	0.044	NS	0.0308	0.0204
Brainstem										
	Actin-related protein 2 isoform 4	gi|73969820	490	0.1348 ± 0.0067	0.1785 ± 0.0249	0.1128 ± 0.0063	0.025	NS	NS	0.0216
	Annexin A6 (Annexin VI) (Lipocortin VI) (P68) (P70) (Protein III) (Chromobindin 20) (67 kDa calelectrin) (Calphobindin-II) (CPB-II) isoform 2	gi|73953627	246	0.0739 ± 0.0071	0.0722 ± 0.0074	0.0456 ± 0.0023	0.0078	NS	0.0127	0.0193
	ATPase, H+ transporting, V1 subunit B, isoform 2 isoform 2	gi|73993820	338	0.3896 ± 0.0345	0.2466 ± 0.0090	0.5235 ± 0.0593	0.0008	NS	NS	0.0005
	ATPase, H+ transporting, V1 subunit B, isoform 2 isoform 2	gi|73993820	341	0.2130 ± 0.0295	0.0973 ± 0.0214	0.2944 ± 0.0141	0.0001	0.0066	NS	0.0001
	Centrosomal protein 63kDa isoform 2	gi|194221623	754	0.1721 ± 0.0061	0.3377 ± 0.0335	0.2202 ± 0.0244	0.0007	0.0006	NS	0.0098
	Chain A, Solution Structure Of The Twelfth Cysteine-Rich Ligand- Binding Repeat In Rat Megalin	gi|159164645	128	0.0365 ± 0.0077	0.0699 ± 0.0118	0.0339 ± 0.0044	0.016	0.0363	NS	0.0241
	Creatine kinase B-type (Creatine kinase, B chain) (B-CK) isoform 1	gi|73964131	508	0.0802 ± 0.0087	0.1289 ± 0.0137	0.0846 ± 0.0072	0.0076	0.0115	NS	0.0209
	Cytosolic purine 5-nucleotidase (5-nucleotidase cytosolic II) isoform 8	gi|73998435	993	0.3931 ± 0.0260	0.6284 ± 0.0636	0.4158 ± 0.0390	0.0041	0.0063	NS	0.0128
	GDP dissociation inhibitor 2	gi|50978926	429	0.1042 ± 0.0063	0.0839 ± 0.0096	0.0335 ± 0.0150	0.0011	NS	0.001	0.0135
	Glutathione S-transferase Mu 3 (GSTM3-3) (GST class-mu 3) (hGSTM3-3) isoform 1	gi|57088159	807	0.1705 ± 0.0128	0.2736 ± 0.0398	0.1591 ± 0.0229	0.0186	0.0452	NS	0.0257

Table 4 (Continue)

	GTP-binding protein alpha o	gi|8394152	550	0.1927 ± 0.0220	0.3018 ± 0.0375	0.1850 ± 0.0118	0.0104	0.0164	NS	0.0248
	Immunoglobulin heavy chain variable region	gi|112700066	1023	0.2323 ± 0.0192	0.4159 ± 0.0349	0.2525 ± 0.0302	0.0007	0.0012	NS	0.0031
	Silent information regulator 2	gi|73697550	566	0.1672 ± 0.0204	0.1711 ± 0.0177	0.0590 ± 0.0072	0.0002	NS	0.0007	0.0005
	Tubulin, alpha 1 isoform 9	gi|73996547	579	0.2392 ± 0.0452	0.5260 ± 0.0861	0.2565 ± 0.0414	0.0074	0.0122	NS	0.0018
	Unidentified	NA	275	0.0747 ± 0.0070	0.0338 ± 0.0020	0.0627 ± 0.0023	0	0	NS	0.0009
	Unidentified	NA	813	0.4906 ± 0.0173	0.3973 ± 0.0308	0.5654 ± 0.0213	0.0006	0.036	NS	0.0004
	Unidentified	NA	1000	0.0931 ± 0.0101	0.1017 ± 0.0117	0.2252 ± 0.0550	0.0216	NS	0.0321	0.0457
Spinal cord										
	40S ribosomal protein S3a (V-fos transformation effector protein) isoform 11	gi|73977917	1394	0.1508 ± 0.0410	0.0887 ± 0.0187	0.2208 ± 0.0126	0.0152	NS	NS	0.0116
	Alpha-crystallin B chain (Alpha(B)-crystallin)	gi|149716488	960	0.5524 ± 0.0525	0.2190 ± 0.0289	0.7896 ± 0.0898	0.0001	0.0054	0.0452	0
	Alpha crystallin B chain (Alpha(B)-crystallin) (Rosenthal fiber component) (Heat-shock protein beta-5) (HspB5) isoform 1	gi|57085977	1385	0.0076 ± 0.0076	0.4507 ± 0.0203	0.1978 ± 0.0448	0	0	0.0011	0.0001
	ATP synthase, H+ transporting, mitochondrial F0 complex, subunit d isoform a	gi|57108097	913	0.3123 ± 0.0156	0.2056 ± 0.0114	0.2918 ± 0.0095	0.0001	0.0001	NS	0.0009
	Carbonic anhydrase I (Carbonate dehydratase I) (CA-I) (Carbonic anhydrase B)	gi|57108007	1395	0.1720 ± 0.0571	0.1475 ± 0.0069	0.0000 ± 0.0000	0.0048	NS	0.0063	0.0178
	Chaperonin containing TCP1, subunit 2 isoform 1	gi|73968673	469	0.1049 ± 0.0087	0.0837 ± 0.0081	0.1453 ± 0.0194	0.0173	NS	NS	0.0146
	Chromosome 1 open reading frame 27	gi|126306536	711	0.1848 ± 0.0194	0.2134 ± 0.0278	0.3747 ± 0.0224	0.0002	NS	0.0003	0.0013
	Collagen, type VI, alpha 1 isoform 1	gi|119887130	1251	0.0041 ± 0.0041	0.0881 ± 0.0190	0.0050 ± 0.0050	0.0006	0.0014	NS	0.0016
	Complement component 1, q subcomponent binding protein precursor	gi|73955331	821	0.3736 ± 0.0209	0.2669 ± 0.0160	0.4236 ± 0.0577	0.027	NS	NS	0.0238
	Creatine kinase B-type (Creatine kinase, B chain) (B-CK) isoform 1	gi|73964131	553	0.6536 ± 0.0330	0.6194 ± 0.0661	0.8821 ± 0.0517	0.011	NS	0.033	0.0144
	Creatine kinase B-type (Creatine kinase, B chain) (B-CK) isoform 1	gi|73964131	579	0.4507 ± 0.0290	0.4179 ± 0.0323	0.6666 ± 0.0596	0.0023	NS	0.0093	0.0033
	Cytoplasmic beta-actin isoform 2	gi|73958067	814	0.0935 ± 0.0197	0.1495 ± 0.0279	0.0139 ± 0.0139	0.0037	NS	NS	0.0028
	Dihydropyrimidinase-like 2	gi|40254595	408	0.2805 ± 0.0384	0.1761 ± 0.0329	0.3310 ± 0.0298	0.0244	NS	NS	0.0212
	Dihydrouridine synthase 1-like (S. cerevisiae)	gi|123288584	1065	0.1881 ± 0.0199	0.1801 ± 0.0299	0.2720 ± 0.012	0.0329	NS	NS	0.0449
	Fructose-bisphosphate aldolase C (Brain-type aldolase) isoform 1	gi|57091277	629	0.4337 ± 0.0392	0.2344 ± 0.0208	0.3765 ± 0.0454	0.0055	0.005	NS	0.0425
	Fructose-bisphosphate aldolase C (Brain-type aldolase) isoform 2	gi|73966974	634	0.0640 ± 0.0110	0.0090 ± 0.0076	0.0703 ± 0.0200	0.0149	0.0381	NS	0.0207
	Glial fibrillary acidic protein, astrocyte (GFAP) isoform 1	gi|73965500	459	0.0620 ± 0.0050	0.0517 ± 0.0032	0.1421 ± 0.0210	0.0003	NS	0.0013	0.0004
	Glial fibrillary acidic protein, astrocyte (GFAP) isoform 1	gi|73965500	602	0.0585 ± 0.0379	0.1897 ± 0.1438	4.3635 ± 0.4024	0	NS	0	0
	Glial fibrillary acidic protein, astrocyte (GFAP) isoform 2	gi|73965502	445	0.0174 ± 0.0059	0.0371 ± 0.0069	0.0000 ± 0.0000	0.0017	NS	NS	0.0012
	Glycogen phosphorylase, muscle form (Myophosphorylase)	gi|1730556	1514	0.0906 ± 0.0323	0.0644 ± 0.0049	0.1619 ± 0.0258	0.0319	NS	NS	0.0304

Table 4 (Continue)

	Heat shock protein 90kDa beta, member 1	gi|50979166	182	0.3857 ± 0.0451	0.3422 ± 0.0475	0.1595 ± 0.0373	0.009	NS	0.0101	0.037
	Heat shock protein beta-1	gi|50979116	1512	0.0000 ± 0.0000	0.1178 ± 0.0105	0.0191 ± 0.0191	0	0	NS	0.0003
	Hypothetical rhabdomyosarcoma antigen Mu-RMS-40.6c	gi|48476968	159	0.0630 ± 0.0070	0.0087 ± 0.0048	0.0411 ± 0.0100	0.0007	0.0005	NS	0.0266
	Isocitrate dehydrogenase 3 (NAD+) alpha isoform 2	gi|73951310	651	0.1590 ± 0.0061	0.1092 ± 0.0059	0.2230 ± 0.0127	0	0.0041	0.0005	0
	Keratin 1	gi|160961491	698	0.1207 ± 0.0148	0.0849 ± 0.0108	0.1658 ± 0.0247	0.0222	NS	NS	0.0173
	Keratin 10 isoform 2	gi|114667513	1381	0.0176 ± 0.0176	0.0756 ± 0.0227	0.3540 ± 0.1066	0.0047	NS	0.0057	0.0205
	Heat shock protein beta-1	gi|50979116	874	0.3965 ± 0.0214	0.3070 ± 0.0141	0.6276 ± 0.0376	0	NS	0.0001	0
	Myotubularin related protein 6	gi|194672062	811	0.1762 ± 0.0133	0.0835 ± 0.0066	0.1628 ± 0.0140	0.0001	0.0002	NS	0.0009
	NADH dehydrogenase (ubiquinone) Fe-S protein 1, 75kDa precursor isoform 1	gi|57110953	283	0.0410 ± 0.0095	0.0402 ± 0.0048	0.0000 ± 0.0000	0.0005	NS	0.0011	0.0013
	N-ethylmaleimide sensitive fusion protein attachment protein beta	gi|62645998	735	0.0988 ± 0.0099	0.1470 ± 0.0457	0.0000 ± 0.0000	0.0155	NS	NS	0.0134
	Oxygen-regulated protein 1; AltName: Full=Retinitis pigmentosa RP1 protein homolog	gi|62900882	157	0.0231 ± 0.0035	0.0000 ± 0.0000	0.0214 ± 0.0071	0.0047	0.0076	NS	0.013
	Peroxiredoxin 2 (Thioredoxin peroxidase 1) (Thioredoxin-dependent peroxide reductase 1) (Thiol-specific antioxidant protein) (TSA) (PRP) (Natural killer cell enhancing factor B) (NKEF-B) isoform 1	gi|73986497	918	0.3579 ± 0.0243	0.2140 ± 0.0242	0.4055 ± 0.046	0.0035	0.0247	NS	0.0035
	rCG47063	gi|149028757	158	0.0375 ± 0.0045	0.0000 ± 0.0000	0.0332 ± 0.0095	0.001	0.0015	NS	0.0042
	Septin-8	gi|73971156	460	0.0907 ± 0.0047	0.0126 ± 0.0106	0.0516 ± 0.0047	0	0	0.0118	0.0118
	Serotransferrin precursor (Transferrin) (Siderophilin) (Beta-1-metal binding globulin) isoform 1	gi|73990142	1220	0.0647 ± 0.0102	0.1730 ± 0.0231	0.0849 ± 0.0173	0.0033	0.0039	NS	0.0166
	Silent information regulator 2	gi|73697550	661	0.1419 ± 0.0139	0.1653 ± 0.0132	0.0792 ± 0.0254	0.0167	NS	NS	0.0158
	Thymopoietin II	gi|229542	1283	0.0000 ± 0.0000	0.1248 ± 0.0057	0.1722 ± 0.0153	0	0	0	0.0091
	Ubiquitin carboxy-terminal hydrolase L1	gi|73951868	872	0.5050 ± 0.0347	0.3185 ± 0.0398	0.5122 ± 0.0482	0.0105	0.0226	NS	0.018
	Unidentified	NA	436	0.0494 ± 0.0051	0.0468 ± 0.0050	0.0092 ± 0.0060	0.0002	NS	0.0005	0.0009
	Werner helicase interacting protein 1, isoform CRA_b	gi|148700412	304	0.0527 ± 0.0031	0.0363 ± 0.0072	0.1077 ± 0.0110	0.0001	NS	0.0008	0.0001
	Zinc finger protein 615	gi|197102729	693	0.1327 ± 0.0094	0.1273 ± 0.0073	0.1698 ± 0.0141	0.0316	NS	NS	0.0394

NCBI = National Center for Biotechnology Information

NA = Not applicable

NS = Not statistically significant

2.3 Characterization of the differentially expressed protein spots

For proteomics identifications through the MASCOT search engine NCBI database, these identified proteins were classified into 11 main categories, namely anti-oxidants, apoptosis-related proteins, cytoskeletal proteins, heat shock proteins/chaperones, immune regulatory proteins, metabolic enzymes, neuron-specific proteins, transcription/translation regulators, ubiquitination/proteasome-related proteins, vesicular transport proteins, and hypothetical proteins.

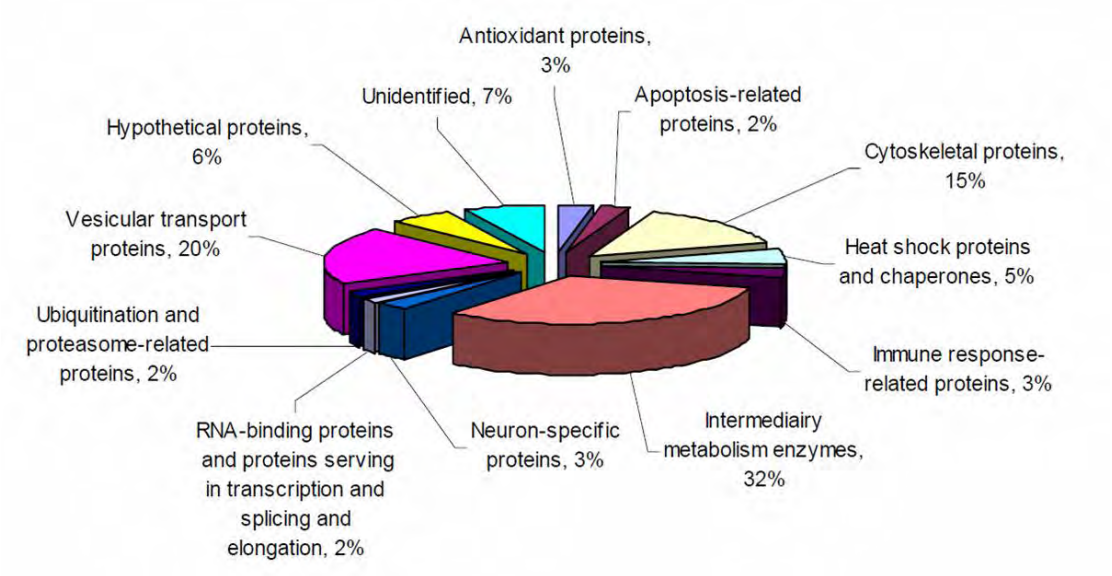

Figure 8. Summary of all differentially expressed proteins in hippocampus, brainstem and spinal cord of dogs naturally infected with rabies. These significantly differed proteins were classified based on their molecular functions. More details of individual proteins, including mass spectrometric data (identities, identification scores, sequence coverage, number of matched peptides, isoelectric point or pI, molecular weight or MW, etc.), quantitative intensity data, and p values obtained from ANOVA as well as Tukey's post-hoc multiple comparisons are summarized in Tables 1-Table 3.

Functional classification of altered proteins in hippocampus, brainstem and spinal cord region compare to non- infected (N), furious (F) and paralytic (D) groups. Altered proteins were identified by mass spectrometric analysis (see Supplementary Table 1-3) and categorized according to their functions based on the NCBI protein database. Note that the spots with the same identities (i.e., post-translationally modified proteins) were counted as only one, and the total number represented the number of unique proteins identified.

Of these 11 main classes, 6 were found of interest in terms of their abundance or locations and/or of clinical types (furious or paralytic) and whether they may play role in pathogenesis (Table 1- Table 3). They are (1). Anti-oxidants (2). Apoptosis-related proteins (3). Cytoskeletal proteins (4). Heat shock proteins/chaperones (5). Immune regulatory proteins (6). Neuron-specific proteins (Table 5).

Table 5: Some interesting changes in furious and paralytic dogs compared to non-infected controls.

Protein name	Spot no.	NCBI ID	Region	Alterations (vs. Control)	
				Paralytic (P)	Furious (F)
Anti-oxidants					
150 kDa oxygen-regulated protein precursor (Orp150) (Hypoxia up-regulated 1)	73	gi|73955046	Spinal cord	↑*	NS
Glutathione S-transferase Mu 3 (GSTM3-3) (GST class-mu 3) (hGSTM3-3) isoform 1	807	gi|57088159	Brainstem	↑*	NS
Oxygen-regulated protein 1; AltName: Full=Retinitis pigmentosa RP1 protein homolog	157	gi|62900882	Spinal cord	↓*	NS
Peroxiredoxin 1	932	gi|4505591	Spinal cord	↓*	↓*
Apoptosis-related proteins					
Annexin A2	1215	gi|18645167	Spinal cord	NS	↓*
Annexin A2	1408	gi|50950177	Spinal cord	↑*	NS
Annexin A6 (Annexin VI) (Lipocortin VI) (P68) (P70) (Protein III) (Chromobindin 20) (67 kDa calelectrin) (Calphobindin-II) (CPB-II) isoform 2	246	gi|73953627	Brainstem	NS	↓*
Annexin A6 (Annexin VI) (Lipocortin VI) (P68) (P70) (Protein III) (Chromobindin 20) (67 kDa calelectrin) (Calphobindin-II) (CPB-II) isoform 2	258	gi|73953627	Hippocampus	NS	↑*
Cytochrome P450 2B12 (CYPIIB12)	192	gi|62639273	Hippocampus	↓*	NS
Cytoskeletal proteins					
Dynamin	164	gi|181849	Hippocampus	↓*	NS
Fascin 1	366	gi|4507115	Brainstem	↓*	NS
Glial fibrillary acidic protein, astrocyte (GFAP) isoform 1	459	gi|73965500	Spinal cord	NS	↑*
Glial fibrillary acidic protein, astrocyte (GFAP) isoform 1	602	gi|73965500	Spinal cord	NS	↑*
Myosin, heavy chain 2, skeletal muscle, adult	208	gi|115947178	Brainstem	↓*	NS
Nebulin-related anchoring protein isoform 2	132	gi|114632883	Brainstem	↓*	↓*
NEFM protein	1185	gi|148342538	Spinal cord	↓*	↑*
Neurofilament, heavy polypeptide 200kDa	37	gi|50979202	Brainstem	↓*	↓*
Septin-8	460	gi|73971156	Spinal cord	↓*	↓*
TUBB2B protein	1000	gi|133778299	Hippocampus	NS	↓*
Tubulin, alpha-1 isoform 9	579	gi|73996547	Brainstem	↑*	NS
Tubulin, alpha-2 chain (Alpha-tubulin 2) isoform 7	623	gi|73996522	Brainstem	↓*	NS
Vinculin (Metavinculin)	1259	gi|73953587	Spinal cord	↑*	↑*
Xin actin-binding repeat containing 2 isoform 1	1260	gi|66841385	Spinal cord	↑*	NS
Heat shock proteins/chaperones					
Alpha-crystallin B chain (Alpha(B)-crystallin)	960	gi|149716488	Spinal cord	↓*	↑*
Alpha crystallin B chain (Alpha(B)-crystallin) (Rosenthal fiber component) (Heat-shock protein beta-5) (HspB5) isoform 1	895	gi|57085977	Brainstem	NS	↑*
Alpha crystallin B chain (Alpha(B)-crystallin) (Rosenthal fiber component) (Heat-shock protein beta-5) (HspB5) isoform 1	1385	gi|57085977	Spinal cord	↑*	↑*
DnaJ (Hsp40) homolog, subfamily C, member 15 (predicted), isoform CRA_b	1055	gi|149050007	Spinal cord	↓*	↓*
Heat shock cognate 71 kDa protein (Heat shock 70 kDa protein 8)	327	gi|123647	Spinal cord	↑*	NS
Heat shock protein 90kDa beta, member 1	96	gi|50979166	Brainstem	↑*	NS
Heat shock protein 90kDa beta, member 1	182	gi|50979166	Spinal cord	NS	↓*
Heat shock protein beta-1	874	gi|50979116	Spinal cord	NS	↑*
Heat shock protein beta-1	1512	gi|50979116	Spinal cord	↑*	NS
Immune regulatory proteins					
Immunoglobulin heavy chain variable region	1023	gi|112700066	Brainstem	↑*	NS
Interferon alpha 4	107	gi|18767673	Hippocampus	NS	↑*
SARM1 protein	1359	gi|114325428	Hippocampus	NS	↑*
Neuron-specific proteins					

Dihydropyrimidinase related protein-2 (DRP-2) (CRMP-2) isoform 6 (Turned on after division, 64 kDa protein) (TOAD-64) (Collapsin response mediator protein 2)	364	gi|73993705	Spinal cord	NS	↓*
Dihydropyrimidinase related protein-2 (DRP-2) (Turned on after division, 64 kDa protein) (TOAD-64) (Collapsin response mediator protein 2) (CRMP-2) isoform 6	314	gi|73993705	Brainstem	↑*	NS
Dihydropyrimidinase related protein-2 (DRP-2) (Turned on after division, 64 kDa protein) (TOAD-64) (Collapsin response mediator protein 2) (CRMP-2) isoform 4	373	gi|73993699	Spinal cord	↓*	↓*
Dihydropyrimidinase related protein-2 (DRP-2) (Turned on after division, 64 kDa protein) (TOAD-64) (Collapsin response mediator protein 2) (CRMP-2) isoform 6	375	gi|73993705	Spinal cord	↓*	↓*
Dihydropyrimidinase related protein-2 (DRP-2) (Turned on after division, 64 kDa protein) (TOAD-64) (Collapsin response mediator protein 2) (CRMP-2) isoform 6	382	gi|73993705	Hippocampus	NS	↑*

NCBI = National Center for Biotechnology Information

↑ = Increased levels as compared to the control (non-infected)

↓ = Decreased levels as compared to the control (non-infected)

* $p < 0.05$ vs. control

3. Confirmation of the result of proteomics analysis at the mRNA level

Some particular genes were chosen to assure the proteomic result using SYBR green real-time PCR. The primer set for the selected target genes are given in Appendix B. These selected genes corresponded to 5 differently expressed proteins; Aconitase 2 (ACO2), Collapsin response mediator protein 2 (CRMP-2), Glial fibrillary acidic protein (GFAP), Heat shock cognate 71 kDa protein (HSP70) and Hypoxia up-regulated 1 (HYOU1). Glyceraldehyde 3-phosphate dehydrogenase (GAPDH) served as an internal control gene. The results were in accord with those of proteomics data.

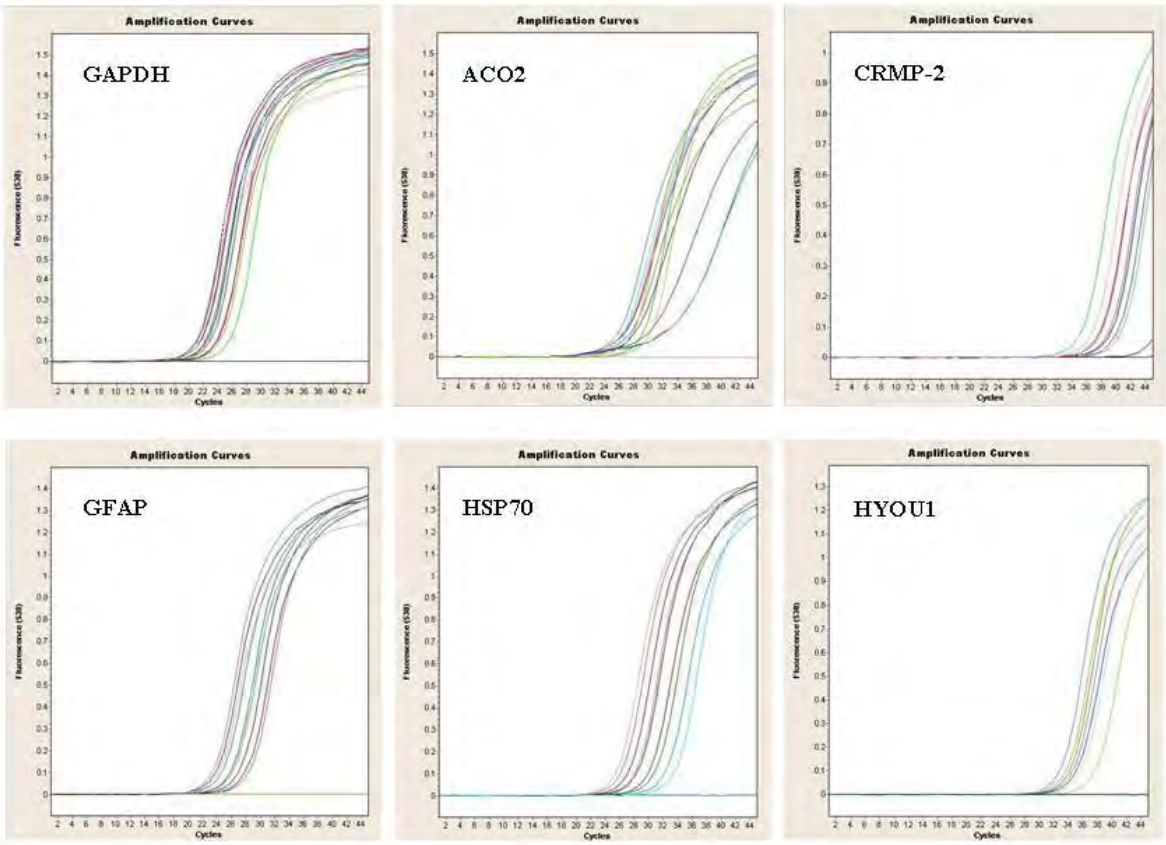

Figure 9. Summary of the cycle number of mRNA levels of 6 genes (GAPDH, ACO2, CRMP-2, GFAP, HSP70 and HYOU1) at which the fluorescence becomes detectable above the background fluorescence.

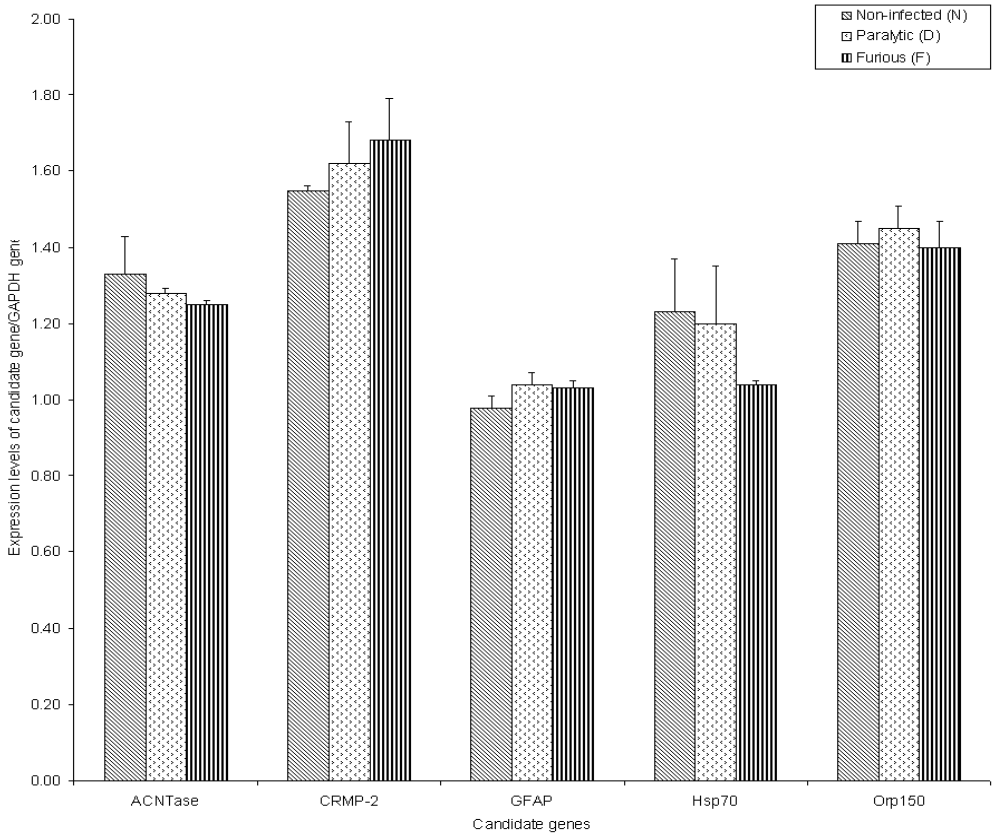

Figure 10. A level of gene expression was analyzed by Q-RT-PCR. Data analysis results are Means±SEM from 5 genes (aconitase 2, CRMP-2, glial fibrillary acidic protein (GFAP), heat shock 70 and hypoxia up-regulated 1) compare to housekeeping gene (GAPDH)

CHAPTER V
DISCUSSION AND CONCLUSION

Natural infection of rabies virus in dog is an ideal animal model for studying the pathogenesis of rabies (Laothamatas et al., 2008). Our results suggest that furious and paralytic rabies infected dogs had differential expression of proteins in their CNS, including hippocampus, brainstem and spinal cord, as compared to the non-infected controls. These proteins were involved in biological processes in response to stress and to the process of rabies viral infection (Figure 8).

Oxidative stress has been reported in rabies (Koprowski, et al., 1993; Hooper et al., 1995; Shin et al., 2004). Axonal swellings with 4-hydroxy-2 nonenal (4-HNE)-labeled puncta, a marker of oxidative stress-dependent lipid peroxidation, were associated with aggregations of activity respiring mitochondria. Jackson and his colleagues have demonstrated that rabies virus infection in cultured DRG neurons derived from adult mice caused axonal injury through oxidative stress (Jackson et al., 2010). Protective proteins (i.e. anti-oxidants) have been shown to be up-regulated to counteract the oxidative stress induced by rabies infection (Zandi et al., 2009). Two isoforms of mitochondrial superoxide dismutase (SOD) were detected on CVS infected BHK cells. *In vivo*, oxidative stress may explain previous observations of the neuronal degeneration processes in the study of transgenic mice that express the yellow fluorescent protein in a subpopulartion of neurons (Scott et al., 2008). In our present study, we found both up- and down-regulations of anti-oxidants in brainstem and spinal cord of paralytic dogs, and down-regulation of one antioxidant protein in the spinal cord of furious dogs (Table 1-3). Thus, emphasizing the importance of oxidative stress injury and may play important role in disrupting tract integrity and cytoskeletal networks as mentioned earlier. In addition, this may suggest autophagy as death process in rabies. Recent study showed numerous autophagic compartments in dorsal root ganglia

neurons infected with CVS in adult mice (Rossiter et al., 2009). These data implicate that the disease process might be at the later stage than anti-oxidants could handle to protect the CNS from oxidative stress (i.e. irreversible deterioration stage). Analysis of the brains at an earlier stage will be helpful to address this hypothesis.

Even with severe clinical entities of both paralytic and furious dogs, there were only 1-2 apoptosis-related proteins that were significantly altered in each region of the CNS, including two forms of annexin A2, two forms of annexin A6, and cytochrome P450 2B12 (CYPIIB12) (Table 1). These data were consistent with previous findings, demonstrating that apoptosis was almost undetectable in wild-type rabies virus infection (Yan et al., 2001; Sarmento et al., 2005; Jackson et al., 2008; Suja et al., 2009; Schnell et al., 2010). Both *in vitro* and *in vivo* observations demonstrate that apoptosis may be a protective rather than a pathogenic mechanism in RV infections because less pathogenic viruses induced more apoptosis than more pathogenic viruses in both *in vitro* and *in vivo* using peripheral routes of inoculation (Morimoto et al.,1999; Yan et al., 2001). Especially, results in this study can be concluded that apoptotic changes in rabies infection depend on many factors such as strain of virus (street, fixed or attenuated strain) and method to detection.

In this study, annexin A2 and A6 were significantly altered in all region of the CNS. From the previous study, annexin XI, V genes were upregulated on day 4, 6 post inoculation with wild type canine rabies virus in suckling mice (Ubol et al., 2006). Annexins are calcium dependent phospholipid-binding proteins and are proposed to act as scaffolding proteins to help direct membrane-membrane and membrane cytoskeleton interactions. In particular, annexin 2 has been shown to bind to actin and be involved in the assembly of actin at cellular membranes (Hayes et al., 2004). Cellular annexin A2 was found to be endogenously associated with HIV, influenza virus particles and VSV virions (Chertova et al., 2006; Shaw et al., 2008; Moerdyk-Schauwecker

et al., 2009). Annexin 2 has been proposed to facilitate HIV-1 assembly at cellular membranes (Chertova et al., 2006). Annexin 2 tightly binds to a member of the S100 family of calcium-binding proteins that promoting fusion events (Lewit-Bentley et al., 2000), and also helps in exocytosis (Gerke et al., 2005). Our study showed that S100 protein, beta chain was successfully identified in natural infection of rabies virus. Other less studied annexin A6 were also identified by our analysis, but their function in the cell is still not clear (Gerke et al., 2005).

The cytoskeleton protein system is closely related to maintaining cell morphology, regulating the progress of protein synthesis, enabling cellular motion, and playing important roles in both intracellular transport and cell division. The obtained data have strongly indicated the important role of the cytoskeleton system in the progress of rabies infection in CNS tissue. Most of cytoskeletal proteins were down-regulated in the CNS of paralytic and furious dogs (Table 1). Decreased amount of cytoskeletal proteins is likely the result of damage by rabies virus infection. These data were consistent with those reported in our previous studies on magnetic resonance imaging of the brains of furious and paralytic dogs during an early stage, which showed tract integrity and macro-structural damage in brainstem of paralytic rabies and in cerebral cortex of furious rabies (Laothamatas et al, in press). This process undoubtedly progresses to further widespread extent once coma ensues. In contrast, two forms of glial fibrillary acidic protein (GFAP), tubulin alpha-1 isoform 9, vinculin and xin actin-binding repeat containing 2 isoform 1 were up-regulated. These increases might be due to reorganization of cytoskeletal assembly in the CNS as a part of host response to the CNS infection. However, as there were much fewer up-regulated proteins, this compensatory mechanism failed to cope with the deterioration of CNS damage by rabies virus.

There are two major mechanisms for protein degradation in eukaryotes: one is the ubiquitin-proteasome pathway and the other is autophagy-lysosome

pathway (Todde et al., 2009). For the ubiquitin system is responsible for protein that targeted to the proteosome for degradation or sent to different locations in the cell (Hochstrasser, 2009). The PPXY motif interacts with ww domain-containing HECT E3 ubiquitin ligase of Nedd4 protein. PPXY motif in Gag of M-PMV, VP40 of Ebola and M protein of rhabdovirus (VSV and RV) provides the structural components. This pathway also participates in virus budding and release (Harty et al., 2001; Ingham et al., 2004).

Autophagy has been proposed as a virus-specific roles relating to viral replication, host innate and adaptive immune responses, virus-induced cell death programs, and viral pathogenesis (Dreux and Chisari, 2010; Levine and Kroemer, 2008). As different virus families and cell types have been shown to display different autophagy responses, it is difficult to make direct comparisons between different virus-cell systems. With respect to anti-viral roles, the autophagy combats infections with viruses by promoting the survival of virally infected cells, and may function by degrading viral components, and/or by activating innate and adaptive immunity. In contrast, some viruses have developed ways to subvert the autophagic machinery for their own benefit in order to avoid the immune response or to increase their viral replication. (Orvedahl and Levine, 2008; Sir and Ou, 2010).

In neurons, highly specialized and post-mitotic long-lived cell types, basal levels of neuronal autophagy may be especially important in neuroprotective. A more recent study in viral encephalitis models, increased autophagy levels in both the herpes simplex virus type 1 (HSV-1) and Sindbis virus has directly correlated with decreased viral titers in infected brains (Liang et al., 1998; Orvedahl et al., 2007). For negative-sense ssRNA virus such as Vesicular stomatitis virus (VSV), deletion of autophagy genes increases viral replication in Drosophila cell lines and decreases Drosophila survival (Shelly et al., 2009).

Although, our results limited change in the autophagy-related protein, more extensive degenerative neuronal changes without the typical features of necrosis or apoptosis in DRG *in vivo* model of experimental rabies virus infection); likely, this neuronal death is due to autophagy (Rossiter et al., 2009). Precise molecular mechanisms governing the cross-talk between autophagy and rabies infected cell remains to be elucidated.

Heat shock proteins or chaperones play important roles in cellular stress responses, protein folding (to ensure the proper protein conformation), and presentation of antigens for the immune system (Latchman, 2004; Pockley, 2003). In rabies, heat shock proteins, especially heat shock protein 70 kDa (Hsp70), are known as the functional molecules for replication found in Negri body, working in concert with Toll-like receptor 3 (TLR3) and ubiquitylated proteins (Sagara and Kawai, 1992; Lahaye et al., 2009; Menager et al., 2009). Our data showed up-regulation of Hsp70 in spinal cord of paralytic dogs. In addition to Hsp70, there were many heat shock proteins or chaperones that were significantly altered in the CNS tissues of both paralytic and furious dogs. However, their levels were either increased or decreased (Table 1-Table 3). These disparate results might be due to the balance between deteriorated effects of virus infection and their counter-balances as the compensatory mechanisms of host to cope with diseases/disorders.

Heat shock cognate 71 kDa protein has previously been shown to be incorporated into rabies, influenza, vesicular stomatitis and Newcastle disease viruses (Sagara and Kawai, 1992) and then proteomics study has been confirmed the presence of Hsp70 within the VSV virions (Moerdyk-Schauwecker et al., 2009). Under noninfectious conditions, HSP70 is known to correct folding of nascent and stress-accumulated misfolded proteins and preventing their aggregation (Hartl et al., 2002), control nuclear import of transcription factors, and directly interact with various components of the tightly regulated programmed cell death machinery, upstream, and downstream

of the mitochondrial events (Ravagnan et al., 2001; Saleh et al., 2000). Finally, HSPs could play a role in the proteasome-mediated degradation of specific cytosolic proteins via chaperone-mediated autophagy (CMA) pathway (Dice, 2007). Heat shock proteins may be potentially involved in all phases of the viral life cycle including cell entry, virion disassembly, viral genome transcription, replication and morphogenesis (Mayer, 2005). For example, the induction of the stress response promoted cytopathic effects of canine distemper virus (CDV) infection and an association of Hsp70 complexes with viral nucleocapsid suggested a possible contribution of HSP70 proteins to viral replication (Oglesbee and Krakowka 1993; Oglesbee et al. 1990).

Collapsin response mediator proteins (CRMPs) form a family of cytosolic phosphoproteins. They are strongly expressed through out the developing nervous system (Charrier et al., 2003). CRMP-2 has been shown to bind to tubulin heterodimers and promotes microtubule assembly, thereby enhancing axonal growth and branching (Fukata et al., 2002). CRMP2 can induce neuronal differentiation in hippocampal cultures (Inagaki et al., 2001). On the other hand, CRMP-2 is also expressed in immune cells and plays a crucial role in T lymphocyte polarization and migration (Vincent et al., 2005). In viral encephalitis in mice, the presence of high CRMP-2 expression in peripheral T lymphocytes associated with high migratory rates for T lymphocytes. This suggests that the activation process may be required for lymphocyte recruitment into the infected brain. CRMP2 expression may serve as indicator of neuroinflamation (Vuaillat et al., 2008). Interestingly, we found CRMP-2 protein at was down-regulated in spinal cord of both paralytic and furious forms of rabies, but was up-regulated in brainstem of paralytic dogs (Table 1).This may be an evidence of in-gressing activated T cells in the brainstem. The fact that inflammatory T cells could be demonstrated only at the brainstem of paralytic rabies (shuangshoti, data unpublished), the infiltrating cells at sites other than brainstem might undergo apoptosis.

There were concordant changes in immune regulatory proteins in CNS tissues of both paralytic and furious dogs. These included up-regulation of immunoglobulin heavy chain in brainstem of paralytic dogs and up-regulations of interferon alpha-4 and SARM1 protein in hippocampus of furious dogs (Table 1). Our data were consistent with the previous findings indicating the involvement of innate immune response in the brain of rabies-infected dogs (Laothamatas et al., 2008).

In addition, we also focused our attention to significant differences between the two forms of rabies in individual CNS tissues, as these data may lead to further identification of tissue biomarkers for differentiation of these two distinct clinical entities of rabies and may also facilitate understanding of factors determining clinical manifestations of rabies. All these significant differences are summarized in Table 4. A total of 13, 17 and 41 proteins in hippocampus, brainstem and spinal cord, respectively, significantly differed between paralytic and furious forms, and thus may potentially be biomarkers to differentiate these two distinct forms of rabies.

It should be noted that there was a previous proteomics study on CVS rabies virus infection in kidney, not neuronal, cells (Zandi et al., 2009). The baby hamster kidney cell line (BHK-21) was infected with CVS rabies virus and alterations in cellular proteome were identified by 2-DE followed by liquid chromatography (LC) coupled to MS/MS. Limited but significant changes were found in expression of viral and host cellular proteins with different functions, including those involved in cytoskeletal assembly, oxidative stress and protein synthesis. Another study was done in rabies-infected mice using 2-DE followed by matrix-assisted laser desorption/ionization time-of-flight (MALDI-TOF) MS (Dhingra et al., 2007). In the latter study, ICR mice were intracerebrally inoculated with attenuated CVS-B2C or wild-type silver-haired bat rabies virus (SHBRV). Animals were sacrificed when they developed severe paralysis and the brains were removed. The expression of host brain proteins, particularly

those involved in ion homeostasis and docking and fusion of synaptic vesicles to presynaptic membranes in the CNS, were altered in the animals infected with SHBRV. On the other hand, attenuated rabies virus CVS-B2C up-regulated the expression of proteins involved in the induction of apoptosis. Comparing the data reported in these two aforementioned studies to ours, not much identical changes was observed. This was not surprising as there were many differences in the study design and models of rabies infection, as well as the affected tissues/cells for proteome analysis. Integrative analysis of several models of rabies virus infection at different stages and in different affected organs/tissues or their locales would be very helpful to obtain the larger and clearer picture of pathophysiology or pathogenic mechanisms of rabies in humans.

Conclusion

In summary, we report herein for the first time a large dataset of changes in proteomes of hippocampus, brainstem and spinal cord in dogs naturally infected with rabies. These data will be useful for better understanding of molecular mechanisms of rabies and for differentiation of its paralytic and furious forms.

REFFERENCES

Akaike, T., et al. Effect of neurotropic virus infection on neuronal and inducible nitric oxide synthase activity in rat brain. **J Neurovirol** 1995; 1(1): 118-125.

Bradford, M.M. A rapid and sensitive method for the quantitation of microgram quantities of protein utilizing the principle of protein-dye binding. **Anal Biochem** 1976; 72: 248-254.

Burdeinick-Kerr, R., Wind, J.,and Griffin, D.E. Synergistic roles of antibody and interferon in noncytolytic clearance of Sindbis virus from different regions of the central nervous system. **J Virol** 2007; 81(11): 5628-36.

Centers for Disease Control and Prevention (CDC). Presumptive abortive human rabies - Texas, 2009. **MMWR Morb Mortal Wkly Rep** 2010; 59: 185-190.

Chang, L.Y., Ali, A.R., Hassan, S.S.,and AbuBakar, S. Human neuronal cell protein responses to Nipah virus infection. **Virol J** 2007; 4: 54.

Charrier, E., et al. Collapsin response mediator proteins (CRMPs): involvement in nervous system development and adult neurodegenerative disorders. **Mol Neurobiol** 2003; 28: 51-64.

Chasserot-Golaz, S.,et al. Annexin 2 promotes the formation of lipid microdomains required for calcium-regulated exocytosis of dense-core vesicles. **Mol Biol Cell** 2005; 16: 1108-1119.

Chertova, E., et al. Proteomic and biochemical analysis of purified human immunodeficiency virus type 1 produced from infected monocyte-derived macrophages. **J Virol** 2006; 80: 9039-9052.

Dacheux, L., et al. A reliable diagnosis of human rabies based on analysis of skin biopsy specimens. **Clin Infect Dis** 2008; 47: 1410-1417.

Dhingra, V., Li, X., Liu, Y.,and Fu, Z. F. Proteomic profiling reveals that rabies virus infection results in differential expression of host proteins involved in ion homeostasis and synaptic physiology in the central nervous system. **J Neurovirol** 2007; 13: 107-117.

Dice, J.F. Chaperone-mediated autophagy. **Autophagy** 2007; 3(4): 295-299.

Dreux, M.,and Chisari, F.V. Viruses and the autophagy machinery. **Cell Cycle** 2010; 9(7): 1295-1307.

Fabis, M.J., Phares, T.W., Kean, R.B., Koprowski, H.,and Hooper, D.C. Blood-brain barrier changes and cell invasion differ between therapeutic immune clearance of neurotrophic virus and CNS autoimmunity. **Proc Natl Acad Sci U S A** 2008; 105(40): 15511-15516.

Fukata, Y., et al. CRMP-2 binds to tubulin heterodimers to promote microtubule assembly. **Nat Cell Biol** 2002; 4: 583-591.

Gerke, V., Creutz, C.E., and Moss, S.E. Annexins: linking Ca^{2+} signalling to membrane dynamics. **Nat Rev Mol Cell Biol** 2005; 6(6): 449–461.

Griffin, D.E. Neuronal cell death in alphavirus encephalomyelitis. **Curr Top Microbiol Immunol** 2005; 289: 57–77.

Guigoni, C.,and Coulon, P. Rabies virus is not cytolytic for rat spinal motoneurons in vitro. **J Neurovirol** 2002; 8: 306-317.

Hartl, F.-U.,and Hayer-Hartl, M. Molecular chaperones in the cytosol: from nascent chain to folded protein. **Science** 2002; 295: 1852–1858.

Harty, R.N., et al. Rhabdoviruses and the cellular ubiquitin-proteasome system: a budding interaction. **J Virol** 2001; 75(22): 10623-10629.

Hattwick, M. A., Weis, T. T., Stechschulte, C. J., Baer, G. M.,and Gregg, M. B. Recovery from rabies. A case report. **Ann Intern Med** 1972; 76: 931-942.

Havert, M.B., Schofield, B., Griffin, D.E.,and Irani, D.N. Activation of divergent neuronal cell death pathways in different target cell populations during neuroadapted sindbis virus infection of mice. **J Virol** 2000; 74(11): 5352-5356.

Hayes, M.J., Rescher, U., Gerke, V.,and Moss, S.E. Annexin-actin interactions. **Traffic** 2004; 5: 571–576.

Hemachudha, T. Human rabies: clinical aspects, pathogenesis, and potential therapy. **Curr Top Microbiol Immunol** 1994; 187: 121-143.

Hemachudha, T., Laothamatas, J.,and Rupprecht, C. E. Human rabies: a

disease of complex neuropathogenetic mechanisms and diagnostic challenges. **Lancet Neurol** 2002; 1: 101-109.

Hemachudha, T.,and Mitrabhakdi, E. Rabies. In Davis, L., and Kennedy, P. G. E (ed). pp 401-444. Oxford: Butterworth-Heinemann, 2000.

Hemachudha, T., et al. Sequence analysis of rabies virus in humans exhibiting encephalitic or paralytic rabies**. J Infect Dis** 2003; 188(7): 960-966.

Hemachudha, T., Wacharapluesadee, S., Laothamatas, J.,and Wilde, H. Rabies. **Curr Neurol Neurosci Rep** 2006; 6(6): 460-468.

Hochstrasser, M. Origin and function of ubiquitin-like proteins. **Nature** 2009; 458(7237): 422-429.

Hooper, D. C., et al. Local nitric oxide production in viral and autoimmune diseases of the central nervous system. **Proc Natl Acad Sci U S A** 1995; 92: 5312-5316.

Inagaki, N., et al. CRMP-2 induces axons in cultured hippocampal neurons. **Nat Neurosci** 2001; 4: 781-782.

Ingham, R.J., Gish, G.,and Pawson, T. The Nedd4 family of E3 ubiquitin ligases: functional diversity within a common modular architecture. **Oncogene** 2004; 23(11): 1972-1984.

Iwata, M., Komori, S., Unno, T., Minamoto, N., and Ohashi, H. Modification of membrane currents in mouse neuroblastoma cells following infection with rabies virus. **Br J Pharmacol** 1999; 126: 1691–1698.

Iwata, M., Unno, T., Minamoto, N., Ohashi, H., and S. Komori. Rabies virus infection prevents the modulation by alpha(2)-adrenoceptors, but not muscarinic receptors, of $Ca(^{2+})$ channels in NG108-15 cells. **Eur J Pharmacol** 2000; 404:79–88.

Jackson, AC. Rabies. **Neurol Clin** 2008; 26(3): 717-726.

Jackson, A. C., Kammouni, W., Zherebitskaya, E.,and Fernyhough, P. Role of oxidative stress in rabies virus infection of adult mouse dorsal root ganglion neurons. **J Virol** 2010; 84: 4697-4705.

Jackson, AC., Park, H. Apoptotic cell death in experimental rabies in suckling mice. **Acta Neuropathol** 1998; 95 (2): 159-164.

Jackson, A.C.,and Park, H. Experimental rabies virus infection of p75 neurotrophin receptor-deficient mice. **Acta Neuropathol (Berl)** 1999; 98(6): 641-644.

Jackson, A.C., Randle, E., Lawrance, G.,and Rossiter, J.P. Neuronal apoptosis does not play an important role in human rabies encephalitis. **J Neurovirol** 2008; 14(5): 368-375.

Jackson, A.C.,and Rossiter, J.P. Apoptosis plays an important role in experimental rabies virus infection. **J Virol** 1997; 71(7): 5603-7.

Jensen, O. N. Modification-specific proteomics: characterization of post-translational modifications by mass spectrometry. **Curr Opin Chem Biol** 2004; 8: 33-41.

Joza, N., et al. Essential role of the mitochondrial apoptosis-inducing factor in programmed cell death. **Nature** 2001; 410(6828): 549–554.

Juntrakul, S., Ruangvejvorachai, P., Shuangshoti, S., Wacharapluesadee, S.,and Hemachudha, T. Mechanisms of escape phenomenon of spinal cord and brainstem in human rabies. **BMC Infect Dis** 2005; 5:104.

Koprowski, H., et al. *In vivo* expression of inducible nitric oxide synthase in experimentally induced neurologic diseases. **Proc Natl Acad Sci U S A** 1993; 90(7): 3024-3027.

Lahaye, X., et al. Functional characterization of Negri bodies (NBs) in rabies virus-infected cells: Evidence that NBs are sites of viral transcription and replication. **J Virol** 2009; 83: 7948-7958.

Laothamatas, J., Hemachudha, T., Mitrabhakdi, E., Wannakrairot, P.,and Tulayadaechanont, S. MR imaging in human rabies. **AJNR Am J Neuroradiol** 2003; 24: 1102-1109.

Laothamatas, J., et al. Furious and paralytic rabies of canine origin: neuroimaging with virological and cytokine studies. **J Neurovirol** 2008; 14: 119-129.

Laothamatas, J., Sungkarat, W.,and Hemachudha, T. Neuroimaging in human rabies. In Jackson, A. C. (ed.). Advances in virus research 79. pp In Press. Academic Press/Elsevier: New York, 2011.

Latchman, D. S. Protective effect of heat shock proteins in the nervous system. **Curr Neurovasc Res** 2004; 1: 21-27.

Lentz, T.L., Burrage, T.G., Smith, A.L., Crick, J.,and Tignor, G.H. Is the acetylcholine receptor a rabies virus receptor? **Science** 1982; 215: 182-184.

Levine, B.,and Kroemer, G. Autophagy in the pathogenesis of disease. **Cell** 2008; 132(1): 27-42.

Lewis, J., Wesselingh, S. L., Griffin, D. E., and Hardwick, J. M. Alphavirus-induced apoptosis in mouse brains correlates with neurovirulence. **J Virol** 1996; 70: 1828–1835.

Lewit-Bentley, A., Réty, S., Sopkova-de Oliveira Santos, J.,and Gerke, V. S100-annexin complexes: some insights from structural studies. **Cell Biol Int** 2000; 24(11): 799-802.

Liang, X.H., et al. Protection against fatal Sindbis virus encephalitis by beclin, a novel Bcl-2-interacting protein. **J Virol** 1998; 72: 8586.

Mayer, M.P. Recruitment of Hsp70 chaperones: a crucial part of viral survival strategies. **Rev Physiol Biochem Pharmacol** 2005; 153: 1-46.

Mayo, M.A.,and Pringle, C.R. Virus Taxonomy. **J Gen Virol** 1997; 79: 649-657.

Menager, P., et al. Toll-like receptor 3 (TLR3) plays a major role in the formation of rabies virus Negri Bodies. **PLoS Pathog** 2009; 5: e1000315.

Mitrabhakdi, E., et al. Difference in neuropathogenetic mechanisms in human furious and paralytic rabies. **J Neurol Sci** 2005; 238: 3-10.

Moerdyk-Schauwecker, M., Hwang, S.I., Grdzelishvili, V.Z. Analysis of virion associated host proteins in vesicular stomatitis virus using a proteomics approach. **Virol J** 2009; 6 :166.

Mori, I., Nishiyama, Y., Yokochi, T.,and Kimura, Y. Virus-induced neuronal apoptosis as pathological and protective responses of the host. **Rev Med Virol** 2004; 14 (4): 209–216.

Morimoto, K., Hooper, D.C., Spitsin, S., Koprowski, H.,and Dietzschold, B.

Pathogenicity of different rabies virus variants inversely correlates with apoptosis and rabies virus glycoprotein expression in infected primary neuron cultures. **J Virol** 1999; 73(1): 510-518.

Murphy, F.A. Rabies pathogenesis. **Arch Virol** 1977; 54(4): 279-297.

Murphy, F.A.,and Bauer, S.P. Early street rabies virus infection in striated muscle and later progression to the central nervous system. **Intervirology** 1974; 3: 256-268.

Murphy, F.A., In Virus Taxonomy : Sixth Report of the International Committee on Taxonomy of viruses. pp 275-288. Springer-Verlag, New York, 1995.

Nargi-Aizenman, J.L.,and Griffin, D.E. Sindbis virus-induced neuronal death is both necrotic and apoptotic and is ameliorated by N-methyl-D-aspartate receptor antagonists. **J Virol** 2001; 75(15): 7114-7121.

Oglesbee, M., and Krakowka, S. Cellular stress response induces selective intranuclear trafficking and accumulation of morbillivirus major core protein. **Lab Investig** 1993; 68: 109–117.

Oglesbee, M., Ringler, S.,and Krakowka, S. Interaction of canine distemper virus nucleocapsid variants with 70 K heat-shock proteins. **J Gen Virol** 1990; 71:1585–1590.

Orvedahl, A.,and Levine, B. Autophagy and viral neurovirulence. **Cell Microbiol** 2008; 10(9): 1747-56.

Orvedahl, A., et al. HSV-1 ICP34.5 confers neurovirulence by targeting the Beclin 1 autophagy protein. **Cell Host Microbe** 2007; 1: 23–35.

Oueslati, A., Fournier, M.,and Lashuel, H. A. Role of post-translational modifications in modulating the structure, function and toxicity of alpha-synuclein: implications for Parkinson's disease pathogenesis and therapies. **Prog Brain Res** 2010; 183: 115-145.

Pockley, A. G. Heat shock proteins as regulators of the immune response. **Lancet** 2003; 362: 469-476.

Préhaud, C., et al. Attenuation of rabies virulence: takeover by the cytoplasmic domain of its envelope protein. **Sci Signal** 2010; 3: ra5.

Préhaud, C., Lay, S., Dietzschold, B.,and Lafon, M. Glycoprotein of nonpathogenic rabies viruses is a key determinant of human cell apoptosis. **J Virol** 2003; 77(19): 10537-10547.

Prosniak, M., Hooper, D.C., Dietzschold, B.,and Koprowski, H. Effect of rabies virus infection on gene expression in mouse brain. **Proc Natl Acad Sci U S A** 2001; 98(5):2758-63.

Ravagnan, L., et al. Heat-shock protein 70 antagonizes apoptosis-inducing factor. **Nat Cell Biol** 2001; 3: 839–843.

Reid, J.E.,and Jackson, A.C. Experimental rabies virus infection in Artibeus jamaicensis bats with CVS-24 variants. **J Neurovirol** 2001; 7(6): 511-517.

Rossiter, J. P., Hsu, L., and Jackson, A. C. Selective vulnerability of dorsal root ganglia neurons in experimental rabies after peripheral inoculation of CVS-11 in adult mice. **Acta Neuropathol** 2009; 118: 249–259.

Sagara, J.,and Kawai, A. Identification of heat shock protein 70 in the rabies virion. **Virol** 1992; 190: 845-848.

Saleh, A., Srinivasula, S. M., Balkir, L., Robbinds, P. D., and Alnemri, E. S. Negative regulation of the Apaf-1 apoptosome by Hsp70. **Nat Cell Biol** 2000; 2: 476–483.

Saikumar, P., et al. Apoptosis: definition, mechanisms, and relevance to disease. **Am J Med** 1999; 107(5): 489–506.

Sarmento, L., Li, X. Q., Howerth, E., Jackson, A. C.,and Fu, Z. F. Glycoprotein-mediated induction of apoptosis limits the spread of attenuated rabies viruses in the central nervous system of mice. **J Neurovirol** 2005; 11: 571-581.

Schnell, M. J., McGettigan, J. P., Wirblich, C.,and Papaneri, A. The cell biology of rabies virus: using stealth to reach the brain. **Nat Rev Microbiol** 2010; 8: 51-61.

Scott, C. A., Rossiter, J. P., Andrew, R. D.,and Jackson, A. C. Structural

abnormalities in neurons are sufficient to explain the clinical disease and fatal outcome of experimental rabies in yellow fluorescent protein-expressing transgenic mice. **J Virol** 2008; 82: 513-521.

Shaw, M.L., Stone, K.L., Colangelo, C.M., Gulcicek, E.E.,and Palese, P. Cellular proteins in influenza virus particles. **PLoS Pathog** 2008; 4: e1000085.

Shelly, S., Lukinova, N., Bambina, S., Berman, A.,and Cherry, S. Autophagy is an essential component of Drosophila immunity against vesicular stomatitis virus. **Immunity** 2009; 30(4): 588–598.

Shin, T., et al. Immunohistochemical localization of endothelial and inducible nitric oxide synthase within neurons of cattle with rabies. **J Vet Med Sci** 2004; 66: 539-541.

Sir, D.,and Ou, J.H. Autophagy in viral replication and pathogenesis. **Mol Cells** 2010; 29(1): 1-7.

Smith, J.S., Fishbein, D.B., Rupprecht, C.E.,and Clark, K. Unexplained rabies in three immigrants in the United States: a virologic investigation. **N Engl J Med** 1991; 324: 205–211.

Suja, M. S., Mahadevan, A., Madhusudhana, S. N., Vijayasarathi, S. K.,and Shankar, S. K. Neuroanatomical mapping of rabies nucleocapsid viral antigen distribution and apoptosis in pathogenesis in street dog rabies--an immunohistochemical study. **Clin Neuropathol** 2009; 28: 113-124.

Thoulouze, M.I., et al. High level of Bcl-2 counteracts apoptosis mediated by a live rabies virus vaccine strain and induces long-term infection. **Virology** 2003; 314(2): 549-561.

Thoulouze, M.I., Lafage, M., Montano-Hirose, J.A.,and Lafon, M. Rabies virus infects mouse and human lymphocytes and induces apoptosis. **J Virol** 1997; 71(10): 7372-7380.

Tirawatnpong, S., et al. Regional distribution of rabies viral antigen in central nervous system of human encephalitic and paralytic rabies. **J Neurol Sci** 1989; 92: 91-99.

Todde, V., Veenhuis, M.,and van der Klei, I.J. Autophagy: principles and significance in health and disease. **Biochim Biophys Acta** 2009; 1792(1): 3-13.

Ubol, S., Hiriote, W., Anuntagool, N.,and Utaisincharoen, P. A radical form of nitric oxide suppresses RNA synthesis of rabies virus. **Virus Res** 2001a; 81(1-2): 125-132.

Ubol, S., Kasisith, J., Mitmoonpitak, C.,and Pitidhamabhorn, D. Screening of upregulated genes in suckling mouse central nervous system during the disease stage of rabies virus infection. **Microbiol Immunol** 2006; 50 (12): 951-959.

Ubol, S., Sukwattanapan, C.,and Maneerat, Y. Inducible nitric oxide synthase inhibition delays death of rabies virus-infected mice. **J Med Microbiol** 2001b; 50(3): 238-242.

Ubol, S., Sukwattanapan, C.,and Utaisincharoen, P. Rabies virus replication induces Bax-related, caspase dependent apoptosis in mouse neuroblastoma cells. **Virus Res** 1998; 56(2): 207-215.

Van Dam, A.M., et al. Appearance of inducible nitric oxide synthase in the rat central nervous system after rabies virus infection and during experimental allergic encephalomyelitis but not after peripheral administration of endotoxin. **J Neurosci Res** 1995; 40(2): 251-260.

Vincent, P., et al. A role for the neuronal protein collapsin response mediator protein 2 in T lymphocyte polarization and migration. **J Immunol** 2005; 175: 7650-7660.

Vuaillat, C., et al. High CRMP2 expression in peripheral T lymphocytes is associated with recruitment to the brain during virus-induced neuroinflammation. **J Neuroimmunol** 2008; 193: 38-51.

Wang, Z.W., et al. Attenuated rabies virus activates, while pathogenic rabies virus evades, the host innate immune responses in the central nervous system. **J Virol** 2005; 79(19): 12554-12565.

Weli, S.C., Scott, C.A., Ward, C.A.,and Jackson, A.C. Rabies virus infection of

primary neuronal cultures and adult mice: failure to demonstrate evidence of excitotoxicity. **J Virol** 2006; 80(20): 10270-10273.

Willoughby, R. E., et al. Survival after treatment of rabies with induction of coma. **N Engl J Med** 2005; 352: 2508-2514.

Wilson, J.M., Hettiarachchi, J.,and Wijesuriya, L.M. Presenting features and diagnosis of rabies. **Lancet** 1975; 2: 1139-1140.

www.cdc.gov/rabies/transmission/virus.html

Yan, X., et al. Silver-haired bat rabies virus variant does not induce apoptosis in the brain of experimentally infected mice. **J Neurovirol** 2001; 7: 518-527.

Zandi, F., et al. Proteomics analysis of BHK-21 cells infected with a fixed strain of rabies virus. **Proteomics** 2009; 9: 2399-2407.

APPENDICES

APPENDIX A

Coated Slides

Protocol

1. Rinse slides 2 changes in acetone.
2. Rinse slides in 2% 3-aminopropyltriethoxysilane 10 sec.
3. Quick rinse in acetone.
4. Rinse in deionized water.
5. Air-dried or in oven.

Immunohistochemistry by Envision™ system (Dako, USA)

Protocol

Slide preparation

1. Cut paraffin embedded tissue thick 3 μm by rotary microtome and put on coated slide.
2. Incubate tissue sections on coated slides 60°C 1 hr.

Deparaffinize tissue section (in a coplin jar)

3. Wash the specimen in 3 changes of xylene, dipping the slide 20 times each in first and second washes, followed by 10 min. in the third wash.
4. Wash the specimen in 3 changes of absolute ethanol, dipping the slide 10 times each in first and second washes, followed by 3 min. in the third wash.
5. Wash the specimen in 3 changes 95% ethanol, dipping the slide 10 times each in first and second washes, followed by 3 min. in the third wash.
6. Wash the specimen one change of distilled water for 1 min.

Antigen retrieval

7. Antigen retrieved by pressure cooker with citrate buffer pH 6.0 1 min.
8. Put the specimen in coplin jar containing PBS for 5 min. at room temp.

Block endogenous peroxidase activity

9. Carefully blot around the section and circle with dako pen (Dako, USA).
10. Apply 3% H_2O_2 in distilled water to completely cover the specimen and incubate in a humidified chamber at room temperature for 10 min.
11. Gently tap excess liquid and wash the specimen with running tap water in a coplin jar for 5 min.
12. Put the specimen in a coplin jar containing PBS 3 min.

Block nonspecific background

13. Apply 3% normal horse serum (NHS) to completely cover the specimen and incubate in a humidified chamber at room temperature for 20 min.

Antibody application

14. Gently tap excess 3% NHS.
15. Apply room temperature primary antibody to the slide to completely cover the specimen and incubated 60 min. in a humidified chamber.
16. Gently tap excess liquid and wash the specimen in 2 changes of PBS in a coplin jar for 3 min. each wash.
17. Apply 1 drop or 200 μl. of visualization reagent (Envision^{TM} system (Dako, USA)) and incubated for 30 min. in a humidified chamber at room temperature.

18. Gently tap off excess liquid and wash the specimen in 2 changes of PBS for 3 min. each wash.

<u>Develop color in peroxidase substrate</u>

19. Apply peroxidase substrate (freshly working DAB) to complete cover the specimen and stain for 10 min. at room temp.
20. Wash the specimen with running tap water in a coplin jar for 3 min.
21. Counterstain with hematoxylin.
22. Mount the specimen under a glass coverslip in a mounting medium (permount).

APPENDIX B

The primer set for the selected target genes are given in Appendix B.

These selected genes corresponded to 5 differently expressed proteins; Aconitase 2 (ACO2), Collapsin response mediator protein 2 (CRMP-2), Glial fibrillary acidic protein (GFAP), Heat shock cognate 71 kDa protein (HSP70) and Hypoxia up-regulated 1(HYOU1). Glyceraldehyde 3-phosphate dehydrogenase (GAPDH) served as an internal control gene.

gene	**forward primer**	**reverse primer**
GAPDH	5′-GGA GAA AGC TGC CAA ATA TG-3′	5′-AGT GGG TGT CAC TGT TGA AGT C-3′
ACO2	5′-AAG TTC CGT GGG CAT CTG-3′	5′-GTG TCA GGG ACA GGA CCA AA-3′
CRMP-2	5′-GGA TGA AGA AGT CCC TGC CT-3′	5′-AGA CAG CGA GTC AAA GTC GAT G-3′
GFAP	5′-ATG GTA CCG GTC CAA GTT CG-3′	5′-TCT CCA GGG ACT CGT TTG TG-3′
HSP70	5′-CGC AAC GTG CTC ATC TTT GA-3′	5′-TTC ACC AGC CTG TTG TCG AA-3′
HYOU1	5′-GGA CCG TGA GGT GCA GTA TCT-3′	5′-TGC TTG GTC ACT GGC ATT G-3′

APPENDIX C

Clustering analysis of the differentially expressed proteins in (A) control, (B) paralysis and furious dog brains, respectively. The rows represent individual proteins. The up- and down-regulated proteins are indicated in red and green, respectively. The intensity of the colors increases as the expression differences increase, as shown in the bar at the top.

APPENDIX D

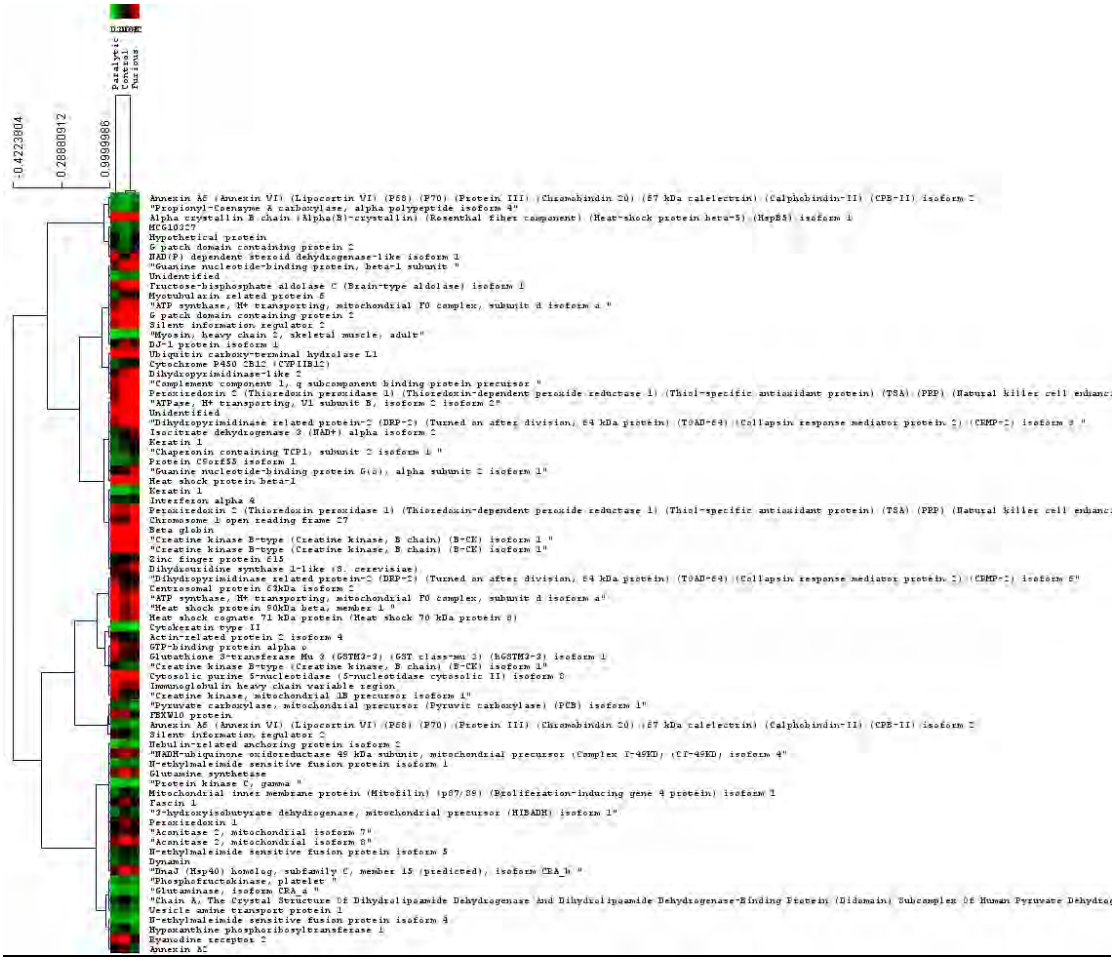

Hierarchical clustering analysis of the differentially expressed proteins in (A) control, (B) paralysis and furious dog brains, respectively. The rows represent individual proteins. The up- and down-regulated proteins are indicated in red and green, respectively. The intensity of the colors increases as the expression differences increase, as shown in the bar at the top.

APPENDIX E

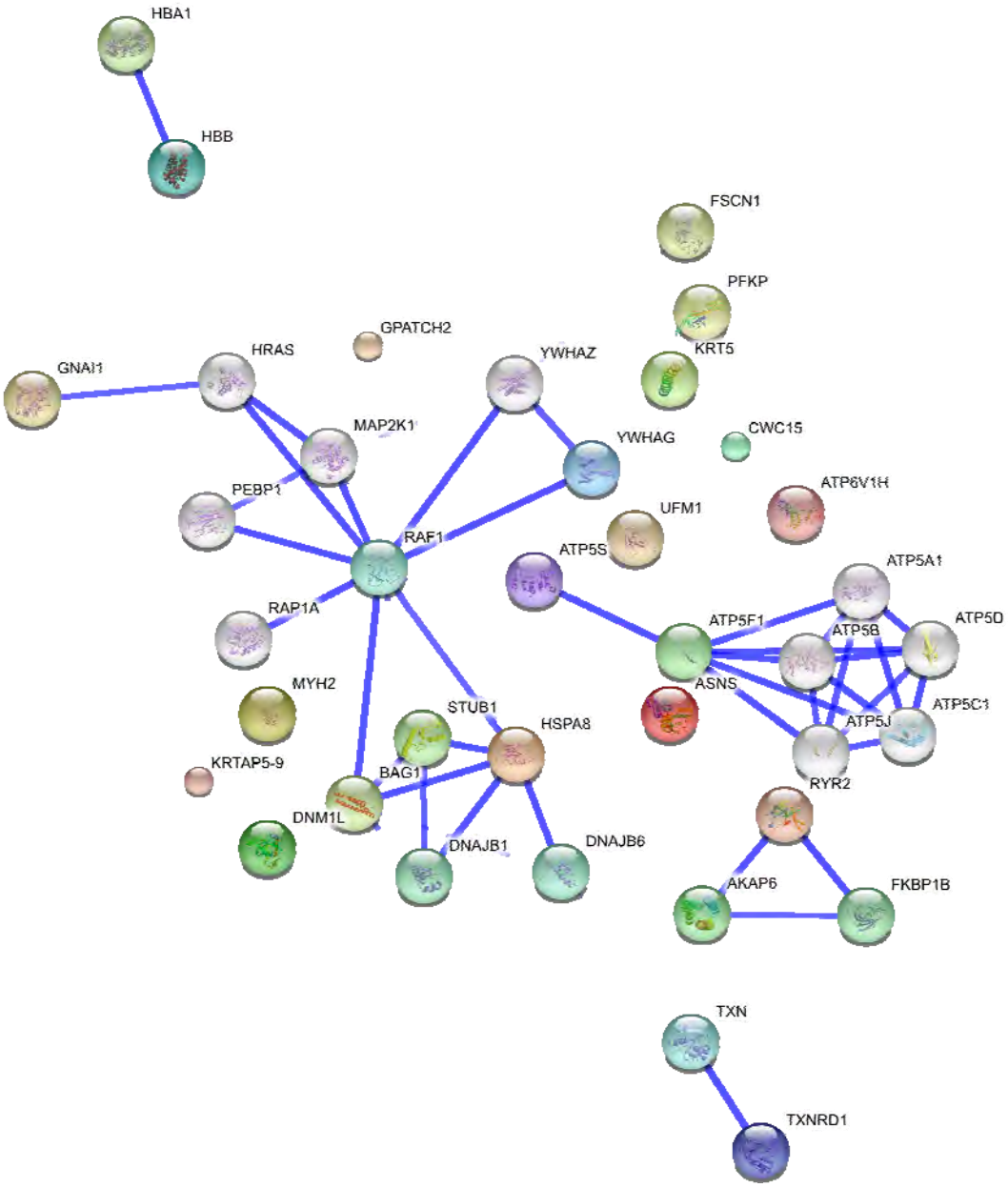

Protein network visualization on the STRING website (http://string-db.org/newstring_cgi/show_input_page.pl?UserId=9VV_DbfDcGEm&sessionId=OuP8CsXmeZ84). The figure shows a composite of two screenshots, illustrating a typical user interaction with STRING.

ASNS	Asparagine synthetase [glutamine-hydrolyzing] (EC 6.3.5.4) (Glutamine- dependent asparagine synthetase) (Cell cycle control protein TS11) (561 aa)
HSPA8	Heat shock cognate 71 kDa protein (Heat shock 70 kDa protein 8); Chaperone. Isoform 2 may function as an endogenous inhibitory regulator of HSC70 by competing the co-chaperones (646 aa)
MYH2	Myosin-2 (Myosin heavy chain 2) (Myosin heavy chain 2a) (MyHC-2a) (Myosin heavy chain, skeletal muscle, adult 2) (Myosin heavy chain IIa) (MyHC-IIa); Muscle contraction. Required for cytoskeleton organization (By similarity) (1941 aa)
KRT5	Keratin, type II cytoskeletal 5 (Cytokeratin-5) (CK-5) (Keratin-5) (K5) (58 kDa cytokeratin) (590 aa)
DNM1L	Dynamin-1-like protein (EC 3.6.5.5) (Dynamin-like protein) (Dnm1p/Vps1p-like protein) (DVLP) (Dynamin family member proline-rich carboxyl-terminal domain less) (Dymple) (Dynamin-related protein 1) (Dynamin-like protein 4) (Dynamin-like protein IV) (HdynIV; Functions in mitochondrial and peroxisomal division probably by regulating membrane fission. Enzyme hydrolyzing GTP that oligomerizes to form ring-like structures and is able to remodel membranes. May also play a role on organelles of the secretory pathway (736 aa)
CWC15	Adrenal gland protein AD-002 (Hypothetical protein HSPC148) (Hypothetical protein ORF5); Involved in pre-mRNA splicing (By similarity) (228 aa)
HBB	Hemoglobin subunit beta (Hemoglobin beta chain) (Beta-globin); Involved in oxygen transport from the lung to the various peripheral tissues (177 aa)
YWHAG	14-3-3 protein gamma (Protein kinase C inhibitor protein 1) (KCIP-1); Adapter protein implicated in the regulation of a large spectrum of both general and specialized signaling pathway.

	Binds to a large number of partners, usually by recognition of a phosphoserine or phosphothreonine motif. Binding generally results in the modulation of the activity of the binding partner (247 aa)
TXNRD1	Thioredoxin reductase 1, cytoplasmic precursor (EC 1.8.1.9) (TR) (TR1); Isoform 1 may possess glutaredoxin activity as well as thioredoxin reductase activity and induces actin and tubulin polymerization, leading to formation of cell membrane protrusions. Isoform 4 enhances the transcriptional activity of estrogen receptors alpha and beta while isoform 5 enhances the transcriptional activity of the beta receptor only. Isoform 5 also mediates cell death induced by a combination of interferon-beta and retinoic acid (651 aa)
ATP5S	ATP synthase subunit s, mitochondrial precursor (ATP synthase coupling factor B) (Mitochondrial ATP synthase regulatory component factor B); Involved in regulation of mitochondrial membrane ATP synthase. Necessary for H(+) conduction of ATP synthase (266 aa)
ATP6V1H	Vacuolar ATP synthase subunit H (EC 3.6.3.14) (V-ATPase H subunit) (Vacuolar proton pump subunit H) (V-ATPase 50/57 kDa subunits) (Vacuolar proton pump subunit SFD) (VMA13) (Nef-binding protein 1) (NBP1); Subunit of the peripheral V1 complex of vacuolar ATPase. Subunit H activates the ATPase activity of the enzyme and couples ATPase activity to proton flow. Vacuolar ATPase is responsible for acidifying a variety of intracellular compartments in eukaryotic cells, thus providing most of the energy required for transport processes in the vacuolar system (By similarity). Involved in the en [...] (483 aa)
KRTAP5-9	Keratin-associated protein 5-9 (Keratin-associated protein 5.9) (Ultrahigh sulfur keratin-associated protein 5.9) (Keratin, cuticle, ultrahigh sulfur 1) (Keratin, ultra high-sulfur matrix protein A)

	(UHS keratin A) (UHS KerA); In the hair cortex, hair keratin intermediate filaments are embedded in an interfilamentous matrix, consisting of hair keratin-associated protein (KRTAP), which are essential for the formation of a rigid and resistant hair shaft through their extensive disulfide bond cross-linking with abundant cysteine residues of hair keratins. The matrix proteins include the h [...] (201 aa)
RYR2	Ryanodine receptor 2 (Cardiac muscle-type ryanodine receptor) (RyR2) (RYR-2) (Cardiac muscle ryanodine receptor-calcium release channel) (hRYR-2); Communication between transverse-tubules and sarcoplasmic reticulum. Contraction of cardiac muscle is triggered by release of calcium ions from SR following depolarization of T- tubules (By similarity) (4965 aa)
GPATCH2	G patch domain-containing protein 2 (528 aa)
UFM1	Ubiquitin-fold modifier 1 precursor; Ubiquitin-like modifier protein which binds to a number of as yet unidentified target proteins (103 aa)
GNAI1	Guanine nucleotide-binding protein G(i), alpha-1 subunit (Adenylate cyclase-inhibiting G alpha protein); Guanine nucleotide-binding proteins (G proteins) are involved as modulators or transducers in various transmembrane signaling systems. The G(i) proteins are involved in hormonal regulation of adenylate cyclase- they inhibit the cyclase in response to beta-adrenergic stimuli (356 aa)
PFKP	6-phosphofructokinase type C (EC 2.7.1.11) (Phosphofructokinase 1) (Phosphohexokinase) (Phosphofructo-1-kinase isozyme C) (PFK-C) (6- phosphofructokinase, platelet type) (784 aa)
FSCN1	Fascin (Singed-like protein) (55 kDa actin-bundling protein) (p55); Organizes filamentous actin into bundles with a minimum of 4.1-1 actin/fascin ratio. Probably involved in the assembly of

actin filament bundles present in microspikes, membrane ruffles, and stress fibers (493 aa)
(Homo sapiens)

BIOLOGRAPHY

Miss Natthapaninee Thanomsridetchai was born in Bangkok, the capital city of Thailand, in April 18th, 1981. In 2003, she received her bachelor degree in Medical Technology from Faculty of Allied Health Sciences, Chulalongkorn University. In 2006, she received her master degree in Medical Sciences from Faculty of Medicine, Chulalongkorn University.

Publication

Agthong, S., Kaewsema, A., Tanomsridejchai, N.,and Chentanez, V. Activation of MAPK ERK in peripheral nerve after injury. **BMC Neurosci** 2006; 7: 45.

Chentanez, V., Thanomsridejchai, N., Duangmardphon, N., Agthong, S., Kaewsema, A., Huanmanop, T., Maneesri, S. Ganglioside GM1 (porcine) ameliorates paclitaxel-induced neuropathy in rats. **J Med Assoc Thai** 2009; 92(1): 50-7.